5-2011

Trace Element Analysis of Rutile and Zr-in-Rutile Thermometry for Southern Appalachian Pelitic Schists

Kathryn A. Eccles
Olivet Nazarene University, flautist22@aol.com

TRACE ELEMENT ANALYSIS OF RUTILE AND ZR-IN-RUTILE THERMOMETRY FOR SOUTHERN APPALACHIAN PELITIC SCHISTS

By

Kathryn A. Eccles

Honors Capstone Project

Submitted to the Faculty of

Olivet Nazarene University

for partial fulfillment of the requirements for

GRADUATION WITH UNIVERSITY HONORS

March, 2011

BACHELOR OF SCIENCE

in

Geology and Science Education

CHARLES CARRIGAN		3/21/11
Capstone Project Advisor (printed)	Signature	Date
Sue E. Williams		4-04-11
Honors Council Chair (printed)	Signature	Date
Janna R. McLean		4/7/11
Honors Council Member (printed)	Signature	Date

To my loving and supportive family and one of my best friends, Jamie Fearon

ACKNOWLEDGMENTS

This project would not have been possible without Charles Carrigan serving as research mentor, GSA abstract coauthor, fieldwork participant, editor, and in many other capacities. Thanks to Tim Eddy for his initial fieldwork with Charles Carrigan and the collection and preparation of one of the samples analyzed. Daniel Bishop deserves thanks for acting as field assistant on the June 2010 fieldwork trip to the southern Appalachians, as does Chris Schkerke for acting as a research assistant on the January 2011 analytical trip to the University of Michigan. Jorden Hayes's company and encouragement while presenting preliminary research at the annual Geological Society of America (GSA) meeting were also invaluable. Additional thanks to Max Reams and Janna McLean for manuscript revisions and input.

Data sets for the project were collected on the Cameca SX-100 Electron Microprobe Analyzer at the University of Michigan Electron Microbeam Analysis Laboratory (EMAL), which is supported by NSF grant #EAR-9911352. Special thanks to Carl Henderson at the University of Michigan EMAL for his immense help with the electron microprobe.

Funding for the project was provided by the Olivet Nazarene University (ONU) Pence Boyce Summer Research fund, an ONU College of Arts and Sciences Research Grant to Charles Carrigan, and an ONU Honors Program Research Grant to Kathryn Eccles. Additional funds from the ONU Pence Boyce fund and a GSA travel grant funded presentation of initial findings in Denver at the GSA annual meeting.

PREFACE

Mountains have long intrigued humans, standing as sentinels above the flatlands and serving as obstacles to be overcome, destinations, or simply sources of inspiration. Most of the pioneers who originally molded the vast, empty wild into a mix of homes and agricultural patchwork amidst remaining natural lands first had to cross at least one range of imposing mountains, facing perils to reach a new future. Over time, people overcame many of the perils associated with the mountains and instead began to flock to the mountains as an escape from the routine living found in cities far below the impressive peaks. Even amidst city living and urban sprawl, the countless images of mountains that have been captured in every art form imaginable preserve the mountains and provide them as a source of inspiration to all.

Over the course of my own life, I have found myself drawn to the mountains. My family spent vacations during my childhood in mountain ranges from Washington to North Carolina. Once I entered college and began exploring my passion for geology, I learned I could use the mountains I love to explore pivotal, unanswered questions about Earth Science. Metamorphic rocks from mountain ranges across the continent can shed light on previously unknown details about Earth's history and processes, such as the mechanism of tectonics and the process of mountain building. Serving as everything from a source of inspiration to an invaluable geological tool, mountains have touched many aspects of academia as well as my own life, leaving their importance clear.

TABLE OF CONTENTS

LIST OF FIGURES

LIST OF TABLES

ABSTRACT

Over the past decade, geochronology studies in the southern Appalachians have focused on zircon, monazite, and mica ages to confirm the occurrence of a major Taconic event (~460-450 Ma) affecting the Western and Central Blue Ridge, followed by a younger NeoAcadian (~360-345 Ma) event affecting the Eastern Blue Ridge and Piedmont. Peak conditions of granulite facies metamorphism are estimated at ~850°C (garnet-biotite) and 7-9 kbar (GASP) for sillimanite schists at Winding Stair Gap (WSG), but thermobarometric studies of metasedimentary rocks in the region are limited and consequently Pressure-Temperature-time-Deformation (P-T-t-D) paths are poorly understood. Many details of the orogenic processes in the region remain unanswered, such as the depth of burial, rates of burial, cooling, and exhumation of various terranes, and variation of ages along strike. Rutile provides a robust, high-temperature U-Pb geochronometer that forms during metamorphic reactions and is a key phase for applying several thermobarometers in the determination of P-T conditions.

This study focuses on electron microprobe analysis of rutile-bearing metapelitic schists in the Blue Ridge to obtain major and some trace element data and the generation of temperature constraints for the orogen. Initial sampling indicates that rutile-bearing schists are somewhat sparse across the orogen, but have been confirmed in the Great Smoky Group of the Western Blue Ridge as well as in the Cartoogechaye and Cowrock terranes of the Central Blue Ridge, all of which were metamorphosed to high grades during the Taconic Orogeny. Rutile is found in both kyanite- and sillimanite-grade rocks, primarily as a matrix phase associated with biotite. Common assemblages in these rocks include garnet, biotite, muscovite, quartz, opaques, plagioclase, ±kyanite, ±sillimanite, and ±staurolite.

Zirconium-in-rutile thermometry performed on the samples generated varying results based on sample location. The thin sections from the Western Blue Ridge were consistent with one another and comparable to previously published temperature estimates of ~600°C, indicating method consistency. However, the samples of Shooting Creek schist from near the Appalachian Trail generated temperatures that were lower than expected, especially since the rutile grains exist as inclusions in the garnet and should represent an earlier, higher-temperature assemblage. Finally, the temperatures for rocks near Winding Stair Gap were much lower than the published peak condition estimates for the area, possibly supporting similar findings from Chen et al. (2007) that temperature estimates may be consistently too low at extreme temperatures and/or pressures due to thermometer resetting.

Keywords**:** rutile, geology, Southern Appalachian Mountains, Winding Stair Gap, zirconium-in-rutile thermometer, zirconium, P-T-t path, geochemistry, geothermobarometry, thermobarometry, electron microprobe

INTRODUCTION

Studying mountain belts is critical to unraveling unanswered questions about how the process of metamorphism changes rocks through burial and uplift, the rates at which mountain building and subsequent erosion occur, and much more. The Appalachian Mountains are one of the notable mountain ranges located within the United States. Stretching from Alabama to the mid-Atlantic seaboard, the southern Appalachians are a portion of the greater Appalachian mountain chain continuing from the southern United States up to Newfoundland, Canada. These mountains have been the subject of many geologic studies, yet retain many secrets.

Many details concerning the orogenic processes in the region remain unanswered, such as the depth of burial, rates of burial, cooling, and exhumation of various terranes, and variation of ages along strike. While some tools such as zircon analysis and GASP barometry have been employed, thermobarometric studies of metasedimentary rocks in the region are limited and consequently Pressure-Temperature-time-Deformation (P-T-t-D) paths are poorly understood. Geologists have begun to focus on the potential for using rutile to add additional constraints to Pressure-Temperature-time conditions, since rutile provides a robust, high-temperature U-Pb geochronometer that forms during metamorphic reactions and is a key phase for applying several thermobarometers in the determination of P-T conditions.

In this study, we endeavor to begin the exploration of the potential usefulness for rutile in the southern Appalachians. This study sought to investigate the availability and geographic distribution of rutile-bearing rocks through research and multiple fieldwork trips. The study also sought to test the method of trace element analysis by specialized operating conditions on an electron microprobe. Finally, the zirconium concentration data gathered was used to calculate temperatures for three different sample areas across the orogen, allowing for petrologic and geographic comparison. Through such analysis, we hoped to demonstrate the potential for trace element analysis of rutile to provide important temperature constraints on metamorphic conditions by comparison to previously published estimates and to begin a larger study focused on answering critical questions about the region.

REVIEW OF LITERATURE

Physical Geology of the Southern Appalachians

The southern Appalachians consist of physiographic provinces that differ in their topography and bedrock. These physiographic provinces divide the Southern Appalachians into three primary regions from northwest to southeast: the Valley and Ridge, the Blue Ridge, and the Piedmont (Fig. 1; Horton and Zullo, 1991).

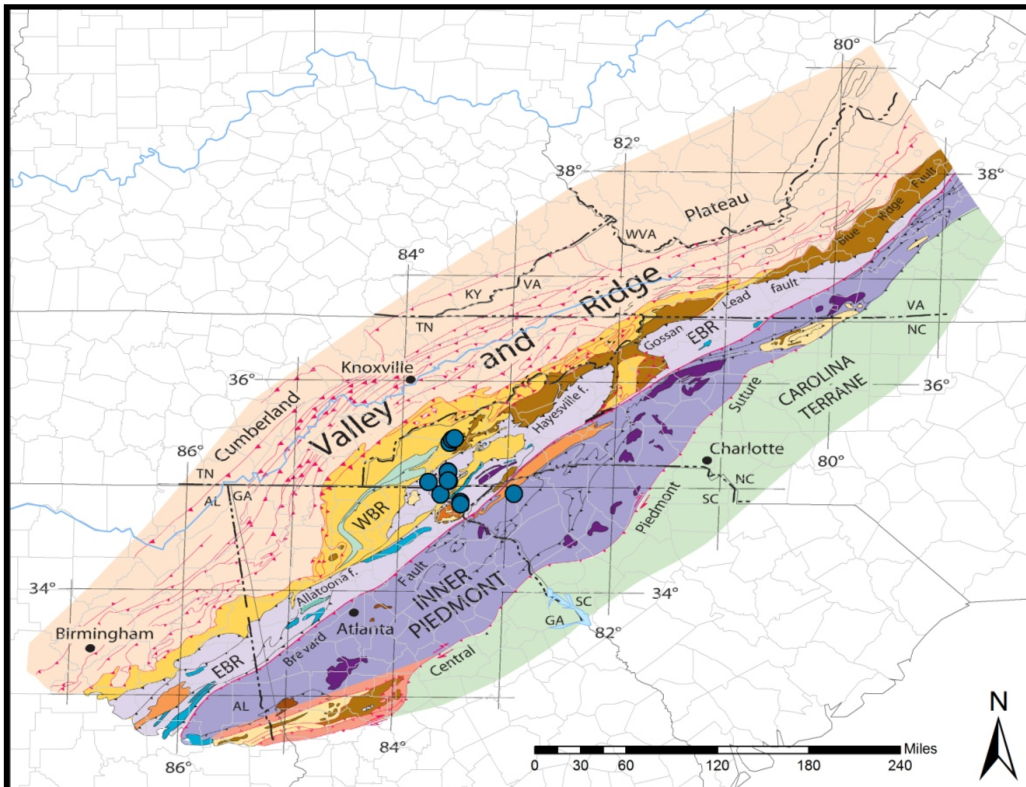

Figure 1: Map of the southern Appalachians highlighting physiographic provinces and tectonic features. Modified from Hatcher et al., 1990.

The Valley and Ridge Province to the northwest contains thick sequences of Paleozoic, unmetamorphosed sedimentary rocks and significant Late Paleozoic thrust faults representing the foreland fold and thrust belt of the Appalachian Orogen (Butler, 1991; Thigpen and Hatcher, 2009). Separated from the Valley and Ridge by the Great Smoky

Thrust is the Blue Ridge, which is the primary modern-day high mountainous area with significant topographic relief and the region of primary interest for this study. Basement Grenvillian gneisses along with younger metamorphic rocks and intrusions are exposed in the Blue Ridge (Hatcher and Goldberg, 1991; Carrigan et al., 2003; Bream et al., 2004). The southeastern province, the Piedmont, is separated from the Blue Ridge by the Brevard Fault Zone and is a relatively flat, high-elevation erosional surface. The majority of the rocks in the Piedmont are Paleozoic, high-grade metamorphic rocks (Horton and McConnell, 1991). To the east, much younger Coastal Plain sediments overlie the Piedmont (Horton and Zullo, 1991).

The bedrock geology in each province is further divided into terranes, defined as internally homogeneous regions that sharply contrast with surrounding areas and from which they are often separated by fault systems (Williams and Hatcher, 1982). They differ from neighboring terranes by stratigraphic package or metamorphic overprinting (Horton and Zullo, 1991). The exact number and names of terranes recognized have varied by researcher and over time, with this discussion following the divisions of Bream and Hatcher (2002).

Historical Geology of the Southern Appalachians

The Appalachian Mountains of the southeastern United States have a long and complicated geologic history that led to the formation of the varying physiographic provinces in the region. The basement rocks, exposed primarily in the Western and Central Blue Ridge, represent tectonic events of the Grenville Orogeny that occurred during the formation of the supercontinent Rodinia from ~1.3 to 0.9 billion years ago

(Horton and Zullo, 1991). These are largely ~1.2-1.1 Ga orthogneisses, with significant variation in age and lithology found in the enigmatic Mars Hill Terrane (Carrigan et al., 2003; Ownby et al., 2004). The break-up of Rodinia ~750-700 million years ago led to the formation of a new continental margin for Laurentia with the opening of the Iapetus Ocean (Horton and Zullo, 1991). As continental drift continued, the newly formed rift margin became a passive margin from the Late Proterozoic to the Cambrian. During the Ordovician, however, the margin again became an active margin as periods of convergence and collision began to occur (Hatcher and Goldberg, 1991). The accretion of continental and oceanic crustal fragments was punctuated by major periods of mountain building activity historically referred to as the Taconic, Acadian, and Alleghanian orogenies (Williams and Hatcher, 1982, 1983; Horton and Zullo, 1991). The crustal fragments accreted to the margin are represented by the differing terranes in the eastern portion of the range. The significance and even existence of each of these historic orogenies, however, has been widely debated. In recent years, geochronologic data have indicated a significant middle Paleozoic event that is younger than the age typically assigned to the Acadian. This has lead many workers to replace the Acadian terminology with the updated term NeoAcadian to signify the younger age (Hatcher et al., 2011).

The Taconic is the first of the three major orogenic cycles to affect the southern Appalachians during the Paleozoic. The event primarily affected the Western and Central portions of the Blue Ridge through high-grade metamorphism and deformation. Zircon and monazite U-Pb data have constrained the timing of the event to ~460 to 450

Ma (Miller et al., 2000; Moecher et al., 2004; Corrie and Kohn, 2007; Merschat et al., 2010). Additional effects are also seen in the Cambro-Ordovician Valley and Ridge sedimentary rocks. Hibbard (2000) has also argued that the effects of the Taconic can be seen in the Piedmont as well, though this remains controversial.

The second major orogenic cycle, the NeoAcadian event, has also been constrained by analysis of zircon U-Pb data (Carrigan et al., 2001; Bream et al., 2004; Merschat et al., 2010). The NeoAcadian event appears to have primarily affected the Eastern Blue Ridge and Inner Piedmont from approximately 360 to 345 Ma, but its areal extent is not fully constrained. However, constraints on the cause and impact of the orogeny have begun to improve over the last five years, with new evidence from geochronology studies and mapping studies indicating the event was likely the result of the docking of the Carolina Superterrane (Hatcher et al., 2011).

The final of the three major cycles, the Alleghanian Orogeny, is well recognized as the last of the three major tectonic events to affect the mountain range. The Alleghanian is considered the result of the collision of Laurentia with Gondwanaland to produce the well-known supercontinent Pangea during the Pennsylvanian through Permian periods of the late Paleozoic (Horton and Zullo, 1991). Evidence for Alleghanian deformation in the southern Appalachians is seen in the multitude of thrust faults throughout the Valley and Ridge (Hatcher and Goldberg, 1991). Additional evidence has been suggested from geochronology studies of metamorphic rocks from the Piedmont and plutons in the Eastern Blue Ridge (Butler, 1991; Miller et al., 2006).

Relevant Blue Ridge Geology

Geology and Tectonics of Blue Ridge Terranes

Terranes and thrust sheets, each containing a unique stratigraphic package, divide the physiographic provinces into smaller, geologically cohesive units. Bream and Hatcher (2002) divide the Blue Ridge into six terranes: the Western Blue Ridge, the Dahlonega Gold Belt, the Cowrock Terrane, the Cartoogechaye Terrane, the Mars Hill Terrane, and the Tugaloo Terrane (Fig. 2).

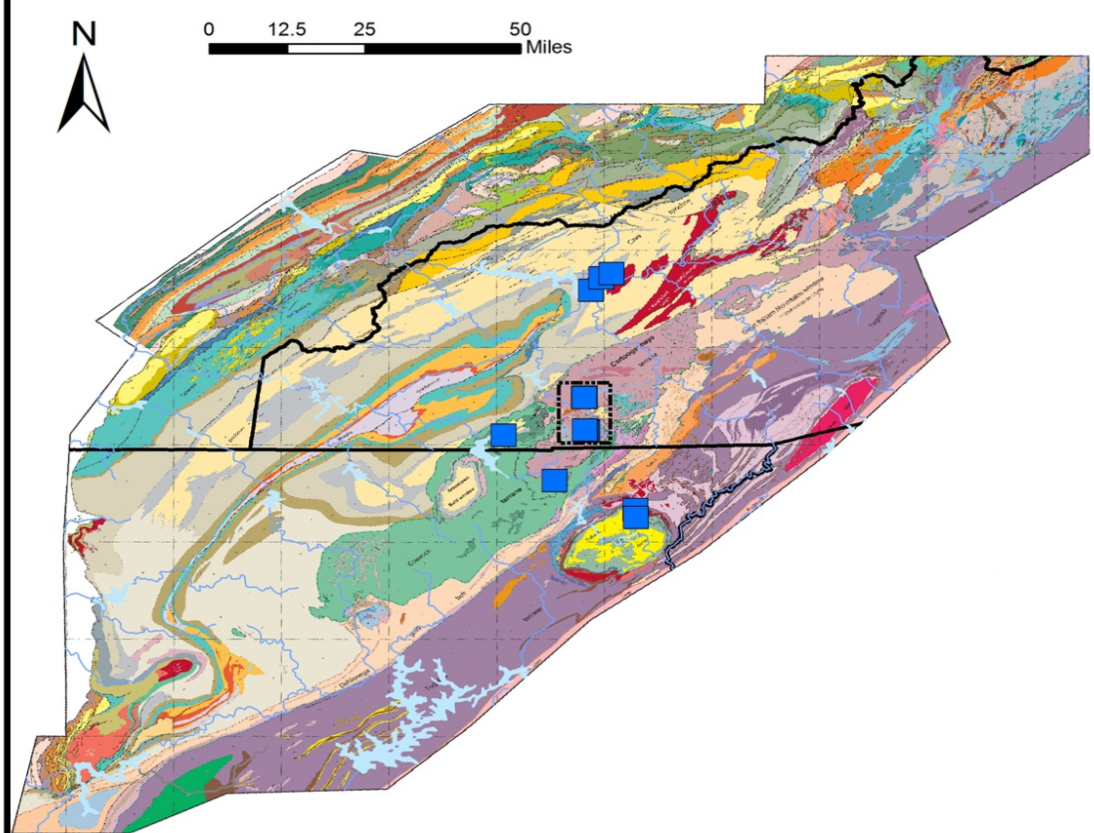

Figure 2: Geologic map of the Blue Ridge, southern Appalachians, showing sample locations. Modified from Thigpen and Hatcher (2009).

The Western Blue Ridge (WBR) is bordered by the Great Smoky Fault to the west, separating it from the Valley and Ridge Province. On the eastern side of the terrane, the WBR is separated from the Dahlonega Gold Belt terrane by the Allatoona fault to the south and from the Cowrock and Cartoogechaye terranes by the Hayesville fault farther north. The Ocoee Supergroup is one of the major stratigraphic units within the Western Blue Ridge. The Ocoee is a thick sequence of metasedimentary rocks that lies unconformably on basement Precambrian gneisses (Thigpen and Hatcher, 2009). Deposition occurred during the late Precambrian as a result of the rifting of Rodinia and formation of the Iapetus Ocean (Hatcher and Goldberg, 1991). Subdivisions of the Ocoee include the Snowbird Group, Great Smoky Group, and the Walden Creek Group.

The Cowrock and Cartoogechaye terranes lie to the east of the WBR across the Hayesville fault. The Hayesville suture separates distinctly North American rocks to the west in the Western Blue Ridge from the suspect terranes to the southeast. Movement along the Hayesville fault has been interpreted to have preceded the metamorphic peak, since metamorphic isograds seem to indicate no significant offset across the fault (Eckert et al., 1989; Eckert and Hatcher, 2003). The Cowrock and Cartoogechaye terranes are separated from one another by the Shope Fork fault. The Cowrock Terrane contains Coweeta Group rocks, while the stratigraphy of the Cartoogechaye Terrane is not yet well defined. It contains metasedimentary rocks that are in some aspects similar to the Coweeta Group and the Tallulah Falls Formation found in the Tugaloo Terrane to the southeast (Hatcher et al., 2003). Within the Cartoogechaye Terrane, along US Highway 64 west of Franklin, North Carolina, at Winding Stair Gap (WSG), is a 370-meter road-cut that exposes the highest-grade metamorphic rocks in the southern Appalachians. The granulite facies metasedimentary and meta-igneous rocks exposed near WSG represent the peak of the southern Appalachian's classic Barrovian sequence and the thermal axis of Taconic metamorphism in the southern Appalachians (Carpenter, 1970; Absher and McSween, 1985; Eckert et al., 1989; Moecher et al., 2004). Figure 3 shows the zones of metamorphism in the southern Appalachians, including the peak conditions near Winding Stair Gap. Rock types reported at WSG include metasedimentary schists, gneisses, and granulites, along with meta-igneous granulites and orthopyroxenites (McSween and Absher, 1984; Absher and McSween, 1985). Deformation at the site likely occurred both during and after peak metamorphism. Moecher et al. (2004) determined the most recent and reliable estimates for peak temperature and pressure conditions of ~850°C by garnet-biotite thermometry and 7 to 9 kbar by garnet-aluminosilicate-quartz-plagioclase (GASP) reaction thermobarometry.

The Dahlonega Gold Belt (DGB) is separated from the Cartoogechaye Terrane to the west by the Soquee River fault and from the Tugaloo Terrane to the east by the Chattahoochee-Holland Mountain fault system. Farther to the south, beyond the southern extent of the Cartoogechaye Terrane, the DGB is juxtaposed against the WBR by the Allatoona fault. The Otto Formation is the main stratigraphic unit within this terrane, with most relationships between the units of the Dahlonega Gold Belt and other terranes remaining uncertain (Thigpen and Hatcher, 2009). Hatcher (pers. comm.) has suggested that it represents a more distal facies of the WBR.

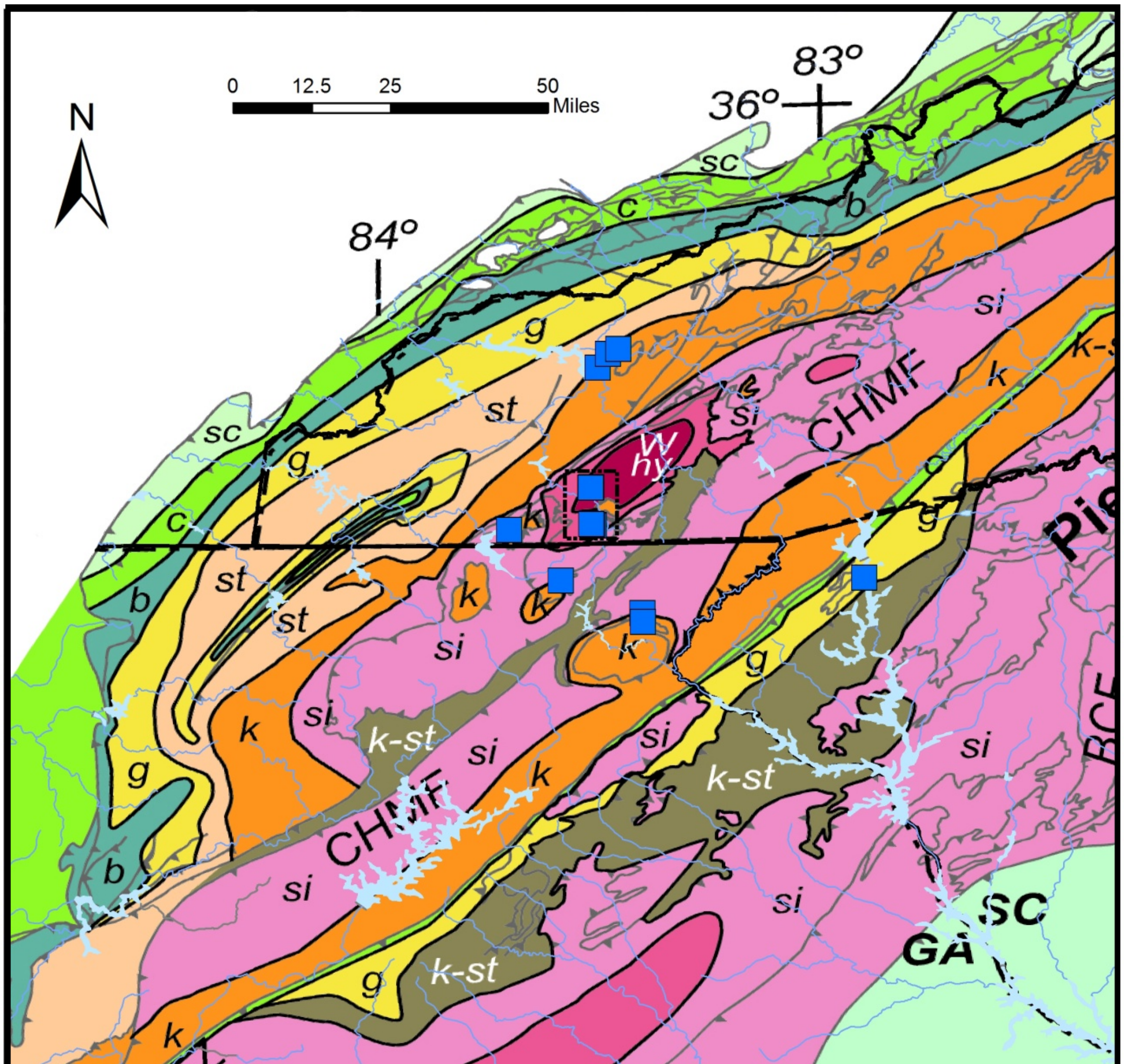

Figure 3: Regional map of a portion of the Blue Ridge and Piedmont physiographic provinces showing metamorphic isograds and sample locations. Modified from Merschat et al., 2010. si=sillimanite; k-st=kyanite-staurolite; g=garnet; k=kyanite; b= biotite; c= chlorite; st=staurolite; hy=hypersthene; CHMF= Chattahoochee-Holland Mountain Fault.

The easternmost terrane of the Blue Ridge is the Tugaloo Terrane. The Tugaloo is bordered by the Chattahoochee-Holland Mountain faults to the northwest. It continues to the southeast and into the Piedmont, and within it lies the Brevard fault zone. The Brevard zone is a wide ductile shear zone separating the Blue Ridge physiographic province from the Inner Piedmont, but it is not regarded as a terrane boundary. The Tallulah Falls-Ashe Formation is the major stratigraphic unit and is composed of high-grade metasandstones, pelitic schists, and amphibolites interpreted as mafic metavolcanic rocks (Thigpen and Hatcher, 2009).

The thrust fault systems in the Blue Ridge have significant offsets, with a minimum displacement of 300 to 500 km toward the interior of the continent. The numerous faults are responsible for the transport of Precambrian basement and metamorphosed Paleozoic rocks in crystalline thrust sheets onto the Paleozoic sedimentary rocks of the Valley and Ridge (Hatcher and Goldberg, 1991).

Blue Ridge Metamorphism

Determining the timing of peak metamorphism and subsequent cooling within mountain ranges is an essential part of understanding the process of mountain building. Several studies have been performed within specific regions of the Appalachians to determine the ages of metamorphism and subsequent cooling. Select ages are summarized in Table 1. A number of age determinations including garnet Sm-Nd mineral isochrons, monazite U-Pb, and multiple zircon U-Pb studies all indicate that the predominant metamorphism of the Blue Ridge is Ordovician ~450-460 Ma (Goldberg and Dallmeyer, 1997; Moecher et al., 2004; Corrie and Kohn, 2007; Merschat et al., 2010). $^{40}Ar/^{39}Ar$ dates on mica and hornblende are distinctly younger across the orogen, suggesting long, slow cooling or thermal reactivation during later events. However, few studies have attempted to combine data using multiple-mineral, thermochronologic and isotopic systems to estimate cooling rates or detect multiple events. To the southeast, a number of U-Pb zircon ages have indicated a second major metamorphic event at ~350

Ma (Carrigan et al., 2001; Merschat et al., 2010). Additionally, very few P-T-t paths have been generated for southern Appalachian rocks and the thermochronologic and thermobarometric estimates of peak temperatures and pressures are limited.

Table 1: Synthesis of important metamorphic dates for the southern Appalachians

Reference	Geochronology Method	Province	Age Determined
Corrie and Kohn, 2007	ID-TIMS U-Pb monazite	Western Blue Ridge	~450 Ma
McClellan et al., 2007	$^{40}Ar/^{39}Ar$ muscovite	Central Blue Ridge	~330 Ma
Carrigan et al., 2001	SHRIMP U-Pb zircon	Eastern Blue Ridge	~350 Ma
Moecher et al., 2004	U-Pb zircon	Eastern Blue Ridge	~460 Ma
Goldberg and Dallmeyer, 1997	Sm-Nd mineral isochron	Blue Ridge	~460 Ma
	$^{40}Ar/^{39}Ar$ hornblende	Blue Ridge	~385 Ma
	$^{40}Ar/^{39}Ar$ muscovite	Blue Ridge	~330 Ma
Merschat et al., 2010	SHRIMP U-Pb zircon	Blue Ridge	~460 Ma (WBR); ~350 Ma (EBR, IP)

Significance of Rutile to Appalachian Tectonics

Occurrence and Composition

Rutile is a fairly common accessory mineral found primarily in medium to high-grade metamorphic rocks, as well as appearing as detritus in sedimentary rocks and very rarely in igneous rocks. High concentrations of rutile are most likely to occur in high-pressure gneisses, schists, amphibolites, and eclogites or as recycled sediments (Deer et al., 1992). Rutile is likely formed in high-pressure rocks by the breakdown of other Ti-rich phases, such as sphene, ilmenite, titanomagnetite, Ti-rich biotite, and possibly others. In addition to TiO_2, rutile may contain trace concentrations of additional elements including Al, V, Cr, Fe, Zr, Mg, Nb, Sn, Sb, Hf, Ta, W, Lu, Mo, Pb, Th and U (Deer et al., 1992; Luvizotto et al., 2009; Meinhold, 2010).

Geochronometer and Geothermobarometer

Rutile's potential for use as a geochronometer and geothermometer has recently garnered increased attention. Multiple methods including electron microprobe analysis (EMPA), thermal ionization mass spectrometry (TIMS), sensitive high-resolution ion microprobe (SHRIMP), and laser ablation inductively coupled plasma mass spectrometry (LA-ICP-MS), have been developed for use with rutile. Examples of applications include the U-Pb dating of metamorphic events (e.g., Mezger et al., 1989; Li et al., 2003), determination of metamorphic temperature conditions (e.g., Spear et al., 2006; Luvizotto and Zack, 2009), and sedimentary provenance studies (e.g., Zack et. al, 2004a; Stendal et al., 2006; Triebold et al., 2007).

Debate concerning the closure temperature of Pb in rutile is ongoing. Some field-based studies, such as Mezger (1989) and Schmitz and Bowring (2003), have placed the closure temperature at 400-450°C. Laboratory studies by Cherniak (2000), however, contend that the closure temperature is much higher, at ~600°C, based on Pb diffusion experiments. Both of these estimates, however, yield values for the closure temperature that are relatively low compared to the closure temperature of Pb in zircon. Due to this lower closure temperature, rutile ages may not indicate the age of peak metamorphism, but rather reflect the post-metamorphic cooling history and could be useful for constraining P-T-t paths (Schmitz and Bowring, 2003).

In addition to its usefulness as a geochronometer, rutile has been used for some time in thermobarometry studies to estimate pressure and temperature conditions during metamorphic events. Mineral assemblages including rutile that are useful in pressure calculations for metapelitic and metamafic rocks include the garnet-rutile-ilmenite-plagioclase-quartz (GRIPS; Bohlen and Liotta, 1986) and garnet-rutile-aluminosilicate-ilmenite-quartz (GRAIL) assemblages (Bohlen et al., 1983). Temperature calculations are primarily achieved using the zirconium-in-rutile geothermometry equations.

The Zr-in-rutile thermometer is based on a strong correlation observed between the incorporation of Zr into rutile and the temperature to which the analyzed grain was exposed (Zack et al., 2004b; Watson et al., 2006; Tomkins et al., 2007). The validity of the calculations are based on the mineral assemblage of rutile-quartz-zircon, as expressed by the balanced equation $SiO_2 + ZrO_{2(\text{in Ru})} = ZrSiO_4$. If quartz is not present, temperature estimates may be overestimations. Systems lacking zircon or that have experienced resetting may underestimate temperatures and only provide minimum temperature values (Zack et al., 2004b). Both zircon and quartz are ubiquitous in most metamorphic rocks, so the full assemblage should be present in almost any metamorphic rock containing rutile. The equations were originally applied to metapelitic rutile, but have since been applied to metamafic and detrital metamafic rutile as well (Zack et al., 2004a; Triebold et al., 2007; Meinhold et al., 2008).

Three different equations for calculating temperatures using the thermometer have been developed. The first equation was developed by Zack et al. (2004b) and was expressed as the formula T(°C)=127.8×ln(Zr_{ppm})-10, with an error of ±50°C (Meinhold, 2010). After the original empirically developed equation based on analysis of natural samples, two additional studies released revised equations. Watson et al. (2006) used experimental data as well as natural samples to generate the formula

$$T(°C) = \frac{4470}{7.36 - \log_{10}(Zr_{ppm})} - 273$$

with an error of ±20°C. The Watson et al. (2006) and the Zack et al. (2004b) equations intersect at approximately 540°C, but are divergent at higher and lower temperatures, indicating that another influence on the system may be present (Meinhold, 2010). As a part of this observation, Tomkins et al. (2007) focused on the potential pressure dependence of Zr uptake in rutile and developed a series of three formulas representing this impact using the stability field of the SiO_2 phase to differentiate the pressure of the system. In the α-quartz field the equation is

$$T(°C) = \frac{83.9 + 0.14 \times P}{0.1428 - R \times \ln(Zr_{ppm})} - 273$$

in the β-quartz field

$$T(°C) = \frac{85.7 + 0.473 \times P}{0.1453 - R \times \ln(Zr_{ppm})} - 273$$

and in the coesite field

$$T(°C) = \frac{88.1 + 0.206 \times P}{0.1412 - R \times \ln(Zr_{ppm})} - 273$$

with R being the gas constant (0.0083144 kJ/K) and the pressure (P) measured in kilobars. The limitation for the Tomkins et al. (2007) equation set is that the pressure under which the rutile originated must be known, making it less than ideal for samples with unknown pressures and detrital samples (Meinhold, 2010).

METHODS

Sample Collection and Initial Processing

Fieldwork

Field sampling for the project occurred in three separate trips. The first sample collection was undertaken by Carrigan and Eddy in July of 2008. Eccles and Carrigan took two additional trips in April and June of 2010. All three trips focused on sampling in the Blue Ridge from different terranes and isograds at locations reportedly containing rutile-bearing rock units. Ten different sites were sampled for a total of twenty-six collected samples to-date. At each outcrop, the sampling procedure involved identification of the desired samples, assignment of sampling codes, obtaining GPS locations for the samples, and taking field pictures and/or measurements. The identification codes assigned to each sample and descriptive information are available in Table 2. Sample location pictures are available in Appendix A.

Map Preparation

The latitude and longitude location data for the sample locations, obtained in the field using handheld GPS units, were checked for accuracy against maps of the areas and then plotted using the ArcGIS software program with georeferenced basemaps. The ArcGIS program was used to produce maps showing the locations of all samples within specific terranes or isograds and to provide a regional understanding of the fieldwork locations. Figure 4 provides an example of one of the maps produced using the ArcGIS program, showing the regional context of several sample locations, along with the geology of the region.

Table 2: Sample descriptions for southern Appalachian fieldwork

ONU Sample ID Code	Latitude			Longitude			Physiographic Province	Terrane	Lithostratigraphic Unit	Comments on location
APRU08-01	35°	7.372'	N	83°	32.559'	W	Eastern Blue Ridge	Cartoogechaye	Shooting Creek Schist	Winding Stair Gap
APRU08-02	34°	54.505'	N	83°	36.804'	W	Eastern Blue Ridge	Cartoogechaye	Unnamed Pelitic Schist (crt)	Sample very close to COLRAB (Bream et al., 2004)
APRU08-03	35°	1.466'	N	83°	43.872'	W	Eastern Blue Ridge	WBR	Copperhill Formation (Great Smoky Group)	Shooting Creek Window
APRU08-04	34°	54.931'	N	82°	54.899'	W	Western Inner Piedmont	Tugaloo	Tallulah Falls Fm.	Sample very close to BPM1; Chauga River Fm.?? (Bream et al., 2004)
APRU08-05	34°	50.04'	N	83°	25.509'	W	Eastern Blue Ridge	Tugaloo	Tallulah Falls Fm.	
APRU08-06	34°	48.839'	N	83°	25.461'	W	Eastern Blue Ridge	Tugaloo	Tallulah Falls Fm.	Tallulah Falls dome, on Rt. 441
APRU10-01:A-B	35°	23.874'	N	83°	31.692'	W	Western Blue Ridge	WBR	Wehutty Formation (Great Smoky Group)	Sample very close to K00-63 (Corrie and Kohn, 2008)
APRU10-02	35°	25.753'	N	83°	30.256'	W	Western Blue Ridge	WBR	Wehutty Formation (Great Smoky Group)	Sample very close to K00-63 (Corrie and Kohn, 2008)
APRU10-03:A-C	35°	26.433'	N	83°	28.851'	W	Western Blue Ridge	WBR	Wehutty Formation (Great Smoky Group)	Sample very close to K00-51 (Corrie and Kohn, 2008)
APRU10-04:A	35°	7.2925485'	N	83°	32.7152343'	W	Central Blue Ridge	Cartoogechaye	Shooting Creek Schist	Winding Stair Gap
APRU10-04:B-D	35°	7.3223988'	N	83°	32.6426002'	W	Central Blue Ridge	Cartoogechaye	Shooting Creek Schist	Winding Stair Gap: several samples
APRU10-04:E-F	35°	7.3494792'	N	83°	32.6012646'	W	Central Blue Ridge	Cartoogechaye	Shooting Creek Schist	Winding Stair Gap: cutting dike
APRU10-05:A	35°	2.139'	N	83°	32.216'	W	Central Blue Ridge	Cartoogechaye	Shooting Creek Schist	on Appalachian Trail, near Standing Indian overlook
APRU10-05:B	35°	2.1230342'	N	83°	32.2554272'	W	Central Blue Ridge	Cartoogechaye	Shooting Creek Schist	on Appalachian Trail, near Standing Indian overlook
APRU10-05:C	35°	2.1977041'	N	83°	32.4404461'	W	Central Blue Ridge	Cartoogechaye	Shooting Creek Schist	along Appalachian Trail
APRU10-05:D	35°	2.3052916'	N	83°	32.5655426'	W	Central Blue Ridge	Cartoogechaye	Shooting Creek Schist	along Appalachian Trail

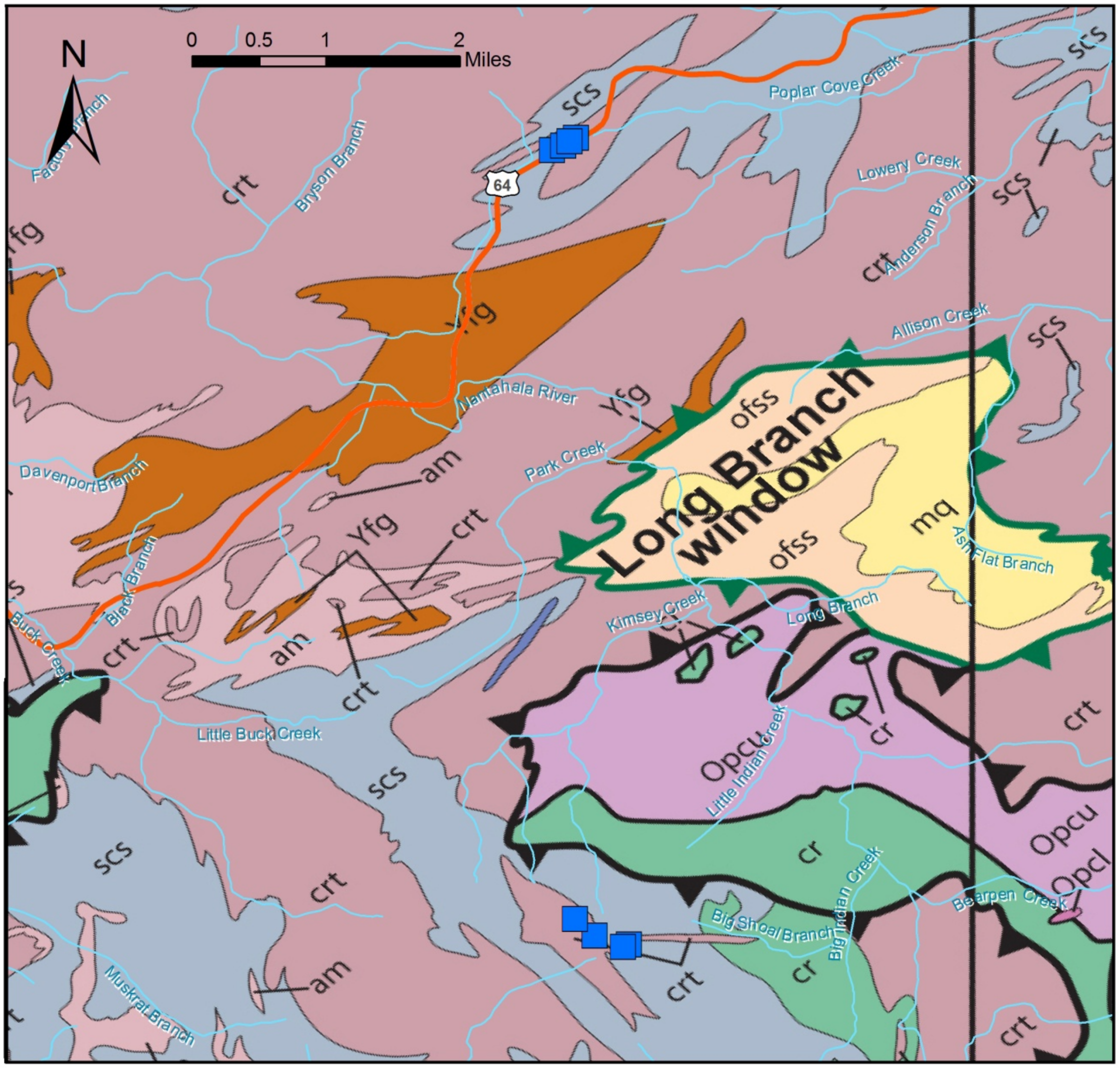

Figure 4: Sample regional map produced using ArcGIS showing sample locations and geology. Basemap from Thigpen and Hatcher (2009).

Sample Analysis

Thin Section Petrography

Rock samples were cut perpendicular to foliation into thin section billets about a third of an inch thick. The billets were sent to Vancouver GeoTech Labs to be prepared into standard polished petrologic thin sections. Thin sections were initially studied using polarized light microscopy to identify the minerals present in each sample and any outstanding textural or compositional characteristics. Special emphasis was placed on identifying samples containing rutile, since further quantitative analysis focused only on those samples. Minerals identified in the samples emphasized in this study are listed in Table 3.

In addition to polarized light microscopy, reflected light was used to create images of the thin sections showing contrasts between grains and the overall thin section texture. Appendix C contains these scanned images, which were notated and used as grain maps during electron microprobe analysis.

Table 3: Petrography of Primary Thin Sections

	APRU08-1	APRU10-1A	APRU10-1B	APRU10-4A	APRU10-4D	APRU10-4E	APRU10-5A	APRU10-5D
Plagioclase Feldspar	X	X	X		X	X	X	
Potassium Feldspar	X							
Quartz	X	X	X	X	X	X	X	X
Biotite	X	X	X	X	X	X	X	X
Muscovite		X	X				X	
Opaques	X	X	X	X		X	X	X (trace Fe-Ti oxide)
Kyanite			X				X	
Sillimanite	X (matrix and garnet)					X (in garnet)	X (in garnet)	X
Rutile	X	X	X	X	X	X	X (in garnet)	X
Garnet	X	X	X		X	X	X	X
Spinel	X					X		
Zircon	X	X	X	X	X	X	X	X
Other	Trace Epidote; malformed carbonate		Staurolite	Opx.	Apatite	Trace apatite	Trace apatite	Graphite

Note: X denotes the detected presence of the specified mineral within the thin section

The Winding Stair Gap samples included two different rock types. The pyroxenite contains orthopyroxene, biotite, quartz, an opaque mineral, and rutile, while the metapelitic schists and gneisses contain quartz, plagioclase, garnet, biotite, an Fe-Ti oxide, rutile, ±spinel, and ±sillimanite. The two Western Blue Ridge samples were taken at a location previously sampled by Corrie and Kohn (2007), who reported rutile within metapelitic schists. The presence of rutile in the WBR rocks was confirmed, as well as plagioclase, quartz, biotite, an Fe-Ti oxide, muscovite, garnet, ±kyanite, and ±staurolite. The final two samples analyzed were from the Cartoogechaye Terrane along a portion of the Appalachian Trail and are metapelitic schists with a mineral assemblage similar to the other schists collected. The Appalachian Trail samples were found to contain rutile, garnet, muscovite, biotite, quartz, ±kyanite, ±sillimanite, and ±graphite. The schists are all fairly similar in their mineral assemblage, but the three different sample locations are at different metamorphic grades and contain different index minerals. The eight thin sections analyzed by electron microprobe were selected as a direct result of the identification of rutile in the slides (Table 3). All samples analyzed contain rutile, garnet, and zircon, the assemblage necessary for application of the Zr-in-rutile thermometer.

Electron Microprobe Analysis

Electron microprobe analysis of the samples was performed at the University of Michigan Electron Microbeam Analysis Laboratory (EMAL). The initial data collection trip was taken during August of 2010, with a second trip to collect additional data points taken in January of 2011.

At EMAL, we used the Cameca SX-100 electron microprobe to analyze the elemental compositions of rutile grains in eight different thin sections. The rutile grains were analyzed using spot analyzes on each grain, with multiple analyses taken when grain size allowed. Elements were standardized using natural and synthetic standards.

Most grains analyzed were also imaged using the backscatter detector (Fig. 5; Appendix D). The locations of spot analyses and rutile grains along with the identification codes assigned to each analytical point were recorded on the grain maps (Appendix C).

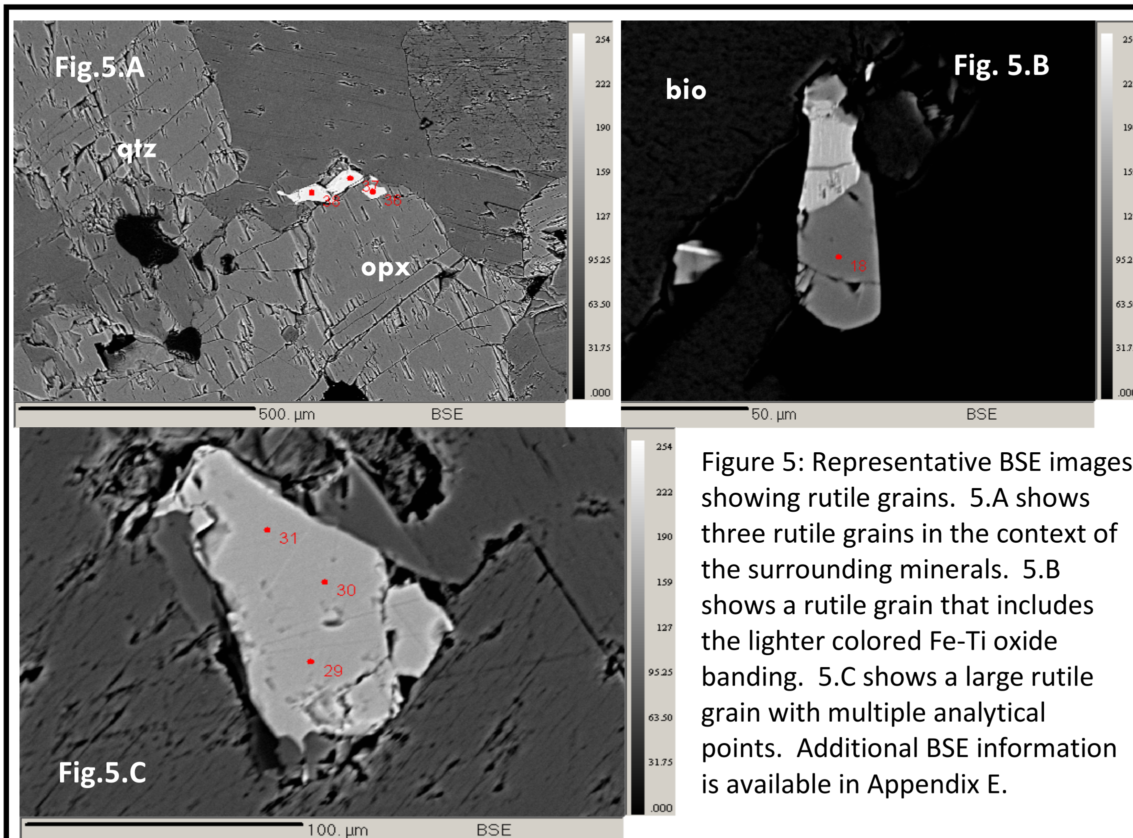

Figure 5: Representative BSE images showing rutile grains. 5.A shows three rutile grains in the context of the surrounding minerals. 5.B shows a rutile grain that includes the lighter colored Fe-Ti oxide banding. 5.C shows a large rutile grain with multiple analytical points. Additional BSE information is available in Appendix E.

The operating conditions for rutile analysis used a 20 µm beam size, counting times of 40 to 180 seconds, a 200 nA beam current, and 25 kV. These conditions were necessary due to the small concentrations of trace elements anticipated, since rutile is generally a fairly pure mineral phase. The trace elements analyzed include Si, Cr, Zr, Nb, and Ta. Zr was measured on two different spectrometers simultaneously and integrated to determine the concentration. V was also analyzed initially, and overlap between V and Ti peaks was corrected by analyzing a V-free rutile standard for V, and then subtracting this amount of apparent V from all other analyses. However, all of the analyses of unknowns yielded negative values of V, indicating that the analyses were overcorrected for V, and have been excluded from the data set. A full listing of the analytical conditions used for rutile analysis for both data collection sessions is available in Appendix E.

From the raw data, calculations were performed to determine the weight percent of each oxide species, the trace element concentration in ppm, the formulas normalized to one cation per formula unit, and the temperatures from the Zr-in-rutile thermometer. The Zr content measured for each analytical point was plugged into the Zr-in-rutile thermometer to generate a temperature value. The equation by Watson et al. (2006),

$$T(°\mathrm{C}) = \frac{4470}{7.36 - \log_{10}(Zr_{ppm})} - 273,$$

was used for the temperature calculations presented by this study. The Watson et al. (2006) equation was chosen over the other two published equations for Zr-in-rutile thermometry since it is a revised version of the equation by Zack et al. (2004b) and since it does not require knowing the pressure conditions for the system, as required by the Tomkins et al. (2007) equation (Meinhold, 2010).

RESULTS

During the course of the two analytical sessions at the University of Michigan, 175 analyses of rutile grains from eight different thin sections were collected. Overall, the rutile grains analyzed were found to be approximately 99 weight percent TiO_2, 0.5 weight percent Fe_2O_3, and the remaining 0.5 weight percent distributed among trace elements. Figures 6.1 through 6.3 show the temperatures calculated for each analytical point plotted to show the distribution of temperatures for each of the three general locations sampled (WBR, WSG, and the Shooting Creek Schist along the Appalachian Trail) and by color-coded thin section. Average values for each sample are shown in Table 4 below, along with standard deviation. Standard deviation indicates the consistency of the samples. Samples having a standard deviation exceeding ±30°C are considered to show significant spread in the data. Representative analyses, including zirconium-in-rutile temperatures, are shown in Table 5. The total data set for the rutile analyses is available in Appendix F.

Table 4: Average Temperature with Standard Deviation for each Sample

	APRU08-1	APRU10-4A	APRU10-4D	APRU10-4E	APRU10-1A	APRU10-1B	APRU10-5A	APRU10-5D
Zr-in-rutile temperature (sample avg. + st. dev.)	554±65	673±20	598±10	631±22	589±9	600±13	623±39	687±24
General Location	Winding Stair Gap				Western Blue Ridge		Cartoogechaye Terrane- Shooting Creek Schist	

Table 5: Representative Analytical Results for Rutile Spot Analyses

	Thin Section:	APRU08-1		APRU10-4A		APRU10-4D		APRU10-4E		APRU10-1A		APRU10-1B		APRU10-5A		APRU10-5D	
	Analytical Point Code:	Ru02-1	Ru09-1	Ru01-1	Ru04-2	Ru05-1	Ru08-2	Ru03-2	Ru05-3	Ru02-2	Ru10-2	Ru01-3	Ru11-1	Ru01-3	Ru03-1	Ru07-2	Ru12-1
Weight Percent	SiO_2	0.014	0.032	0.035	0.021	0.016	0.036	0.042	0.02	0.018	0.02	0.022	0.037	-0.005	0.049	0.001	0.001
	TiO_2	99.376	98.036	97.773	98.269	97.726	100.407	98.87	100.321	99.898	98.043	98.888	99.788	99.741	97.608	99.7	99.448
	ZrO_2	0.008	0.043	0.083	0.053	0.025	0.031	0.043	0.054	0.024	0.027	0.029	0.032	0.07	0.026	0.094	0.061
	Nb_2O_5	0.031	0.138	0.241	0.198	0.662	0.493	0.19	0.327	0.661	0.598	0.552	0.537	0.39	0.378	0.521	0.459
	Ta_2O_5	0.007	0.008	0.009	0.005	0.011	0.014	0.005	0.004	0.026	0.022	0.013	0.024	0.022	-0.002	0.004	0.009
	FeO	0.661	0.602	0.48	0.241	1.011	0.625	0.374	0.712	0.44	0.422	0.274	0.262	0.617	0.938	0.355	0.354
	Cr_2O_3	0.04	0.061	0.461	0.494	0.006	0.007	0.045	0.043	0.06	0.053	0.059	0.055	0.033	0.043	0.059	0.042
	Zr-in-rutile Temperature	513°C	630°C	685°C	647°C	589°C	603°C	630°C	646°C	585°C	595°C	599°C	606°C	669°C	592°C	695°C	658°C

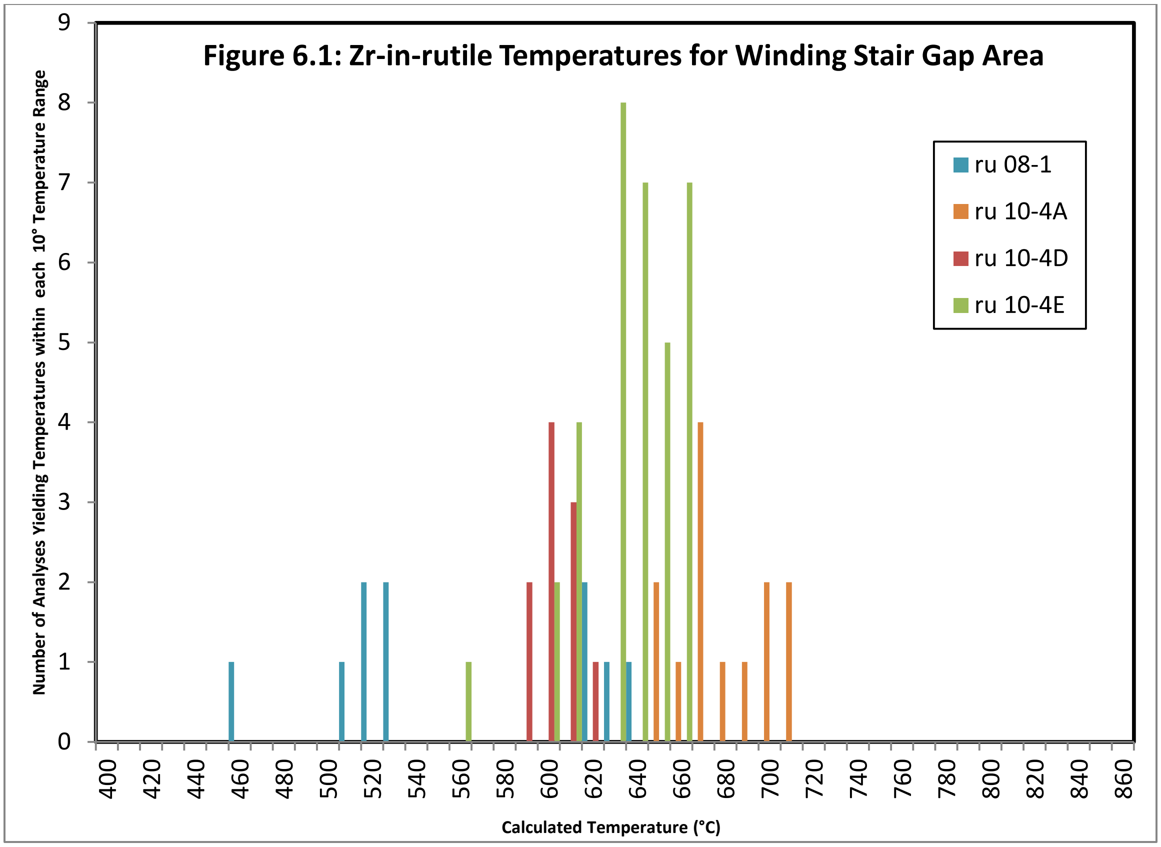
Figure 6.1: Zr-in-rutile Temperatures for Winding Stair Gap Area
ru 08-1
ru 10-4A
ru 10-4D
ru 10-4E
Number of Analyses Yielding Temperatures within each 10° Temperature Range
Calculated Temperature (°C)
0
1
2
3
4
5
6
7
8
9
400
420
440
460
480
500
520
540
560
580
600
620
640
660
680
700
720
740
760
780
800
820
840
860

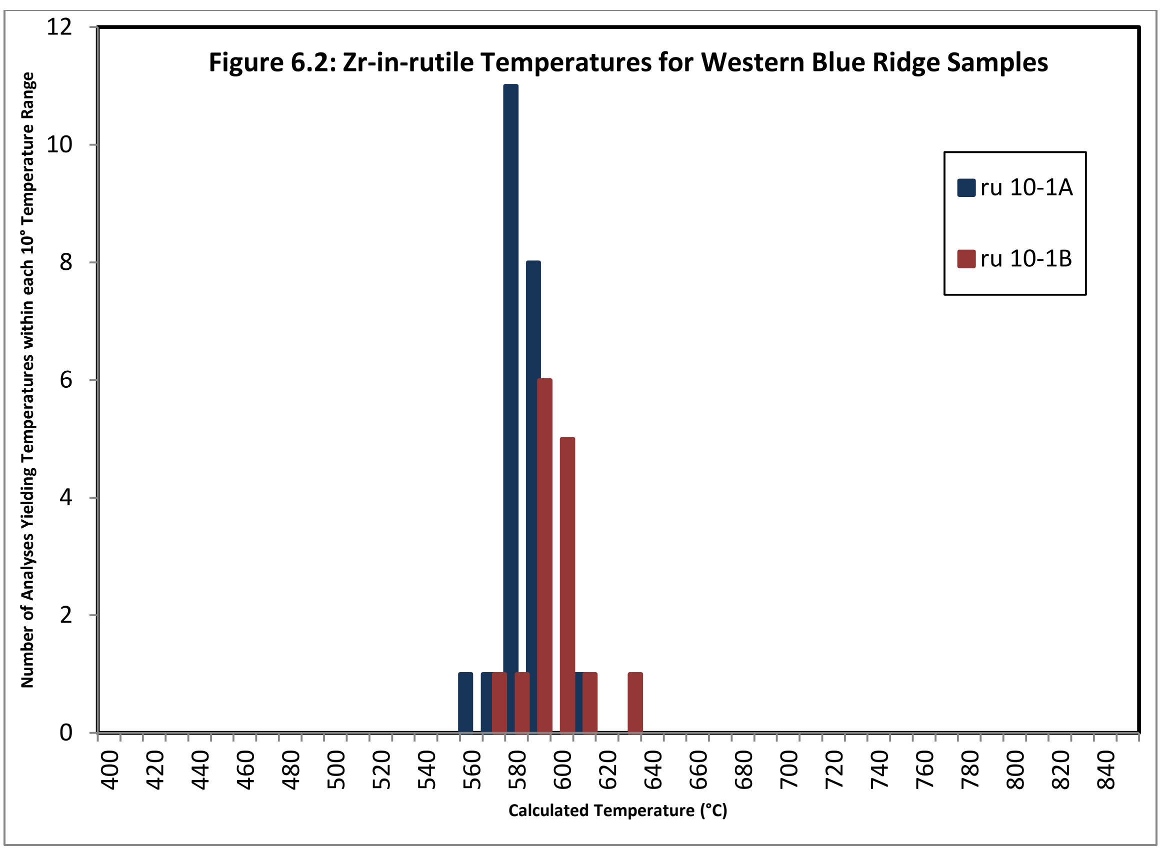
Figure 6.2: Zr-in-rutile Temperatures for Western Blue Ridge Samples
ru 10-1A
ru 10-1B
Number of Analyses Yielding Temperatures within each 10° Temperature Range
Calculated Temperature (°C)
0
2
4
6
8
10
12
400
420
440
460
480
500
520
540
560
580
600
620
640
660
680
700
720
740
760
780
800
820
840

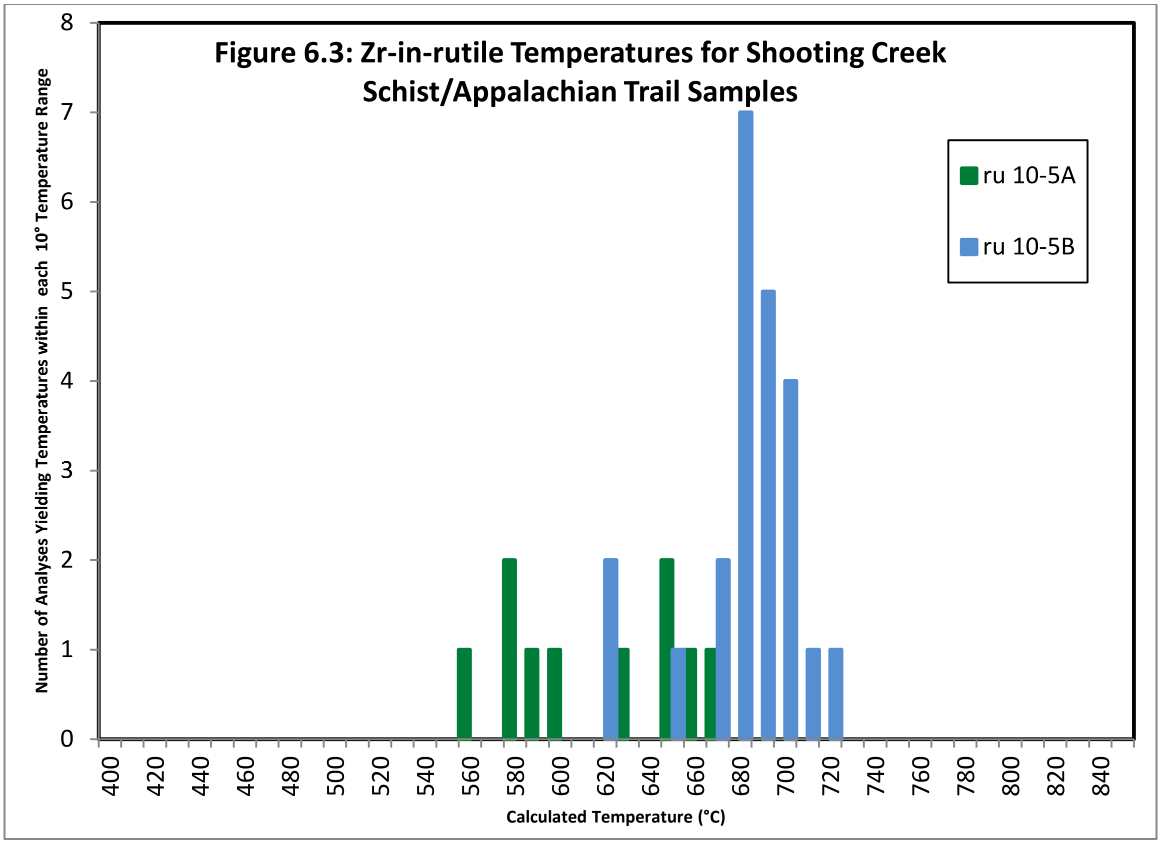

Figure 6: Figures 6.1-6.3 show the distribution of calculated temperatures by sampling location and thin section. Figure 6.1 shows samples collected in the Winding Stair Gap area, with rocks reaching granulite metamorphic conditions and representing the thermal axis of metamorphism (Absher and McSween, 1985). Figure 6.2 shows the two samples analyzed that were collected in the Western Blue Ridge near Great Smoky Mountain National Park. Figure 6.3 plots the two samples of Shooting Creek Schist collected along a portion of the Appalachian Trail near Standing Indian Mountain in the Cartoogechaye Terrane.

DISCUSSION

The Zr-in-rutile temperatures generated from the electron microprobe data indicate considerable agreement with previously published temperature estimates for some samples, and yet considerable divergence for others. The Western Blue Ridge samples were by far the most consistent with each other and with previously published temperature estimates. The two samples generated average temperatures of 589 ±9°C for sample APRU10-1A and 600 ±13°C for sample APRU10-1B. Given that the samples are both mica schists collected from the same outcrop, the similarity of results and overlap of standard deviation ranges is not surprising. The temperatures are also quite similar to peak temperature estimates for kyanite-bearing schists in the vicinity. Mohr and Newton (1983) determined peak temperatures of 580±35°C, and similar results of 590°C and 630°C were determined by Kohn and Malloy (2004).

The mineral assemblage present in the rocks can also be used to provide a general indication of the temperature conditions that likely affected a given rock unit. According to Spear (1995), mineral assemblage identification can constrain the possible temperature range by distinguishing mineral stability fields and metamorphic grade, which are associated with specific metamorphic conditions. For the Western Blue Ridge samples, a temperature range of roughly 550°C to 625°C can be estimated using a P-T grid for the KFMASH system for samples containing kyanite, garnet, and staurolite. These constraints, along with previously published temperature estimates by Mohr and Newton (1983) and Kohn and Malloy (2004), yield values comparable to the temperatures generated by this study. These results verify that the method can be successfully applied to determine estimates of peak metamorphic temperature in staurolite-kyanite grade metapelitic rocks that do not show significant evidence for later recrystallization.

The samples from the Cartoogechaye Terrane (Shooting Creek Schist) are quite distinct from one another petrographically. One of the samples from this location, APRU10-5A, contains rutile as inclusions within large garnet grains but rutile is absent from the matrix. The assemblage within the garnets consists of sillimanite, biotite, ilmenite, and rutile, while the matrix is dominated by kyanite, muscovite, biotite, ilmenite, and plagioclase. Based on the different aluminosilicate phases, we interpret the inclusion assemblage as an earlier, higher-grade assemblage and the matrix as a recrystallization assemblage at slightly lower but still high-grade conditions. Alternatively, the matrix assemblage could be interpreted as a higher pressure assemblage based on the aluminosilicate phase, although the lack of rutile in the matrix suggests otherwise. The second sample, APRU10-5D, contains both abundant rutile and sillimanite in the matrix, lacks muscovite, and does not show the same signs of later recrystallization. The inclusion assemblage in sample 10-5A is noticeably similar to the matrix assemblage of 10-5D. However, the analyses of the included rutile grains in sample 10-5A yield temperatures that are significantly lower than those from grains in the matrix of sample 10-5D. For sample APRU10-5A, the temperatures generated vary between garnet host grains, show significant spread across the sample from 560°C up to 670°C, and the sample has an overall average of 623 ±39°C. The matrix rutile grains from sample APRU10-5D are much more consistent across the sample and yield an average temperature of 687 ±24°C.

Temperature estimates for the system based on a KFMASH system P-T grid for metapelitic rocks indicate that the Shooting Creek Schist samples should have temperatures roughly between 550°C and 650°C for the kyanite-grade matrix of APRU10-5A and temperatures exceeding 700°C for second sillimanite-grade garnet inclusions in the same sample and for all of sample APRU10-5D (Spear, 1995). Calculated temperature results are slightly low compared to the expected high-temperature estimates for sample APRU10-5D. Calculated temperatures for rutile inclusions within the garnet of APRU10-5A also include temperature estimates lower than the values expected for the sillimanite inclusion assemblage and much closer to conditions expected for the kyanite-rich matrix. This suggests that the rutile grains were at least partially reset with respect to Zr concentration during the later recrystallization event, even though they were included within garnet grains.

The temperatures generated for the four Winding Stair Gap thin sections are somewhat variable and significantly lower than published peak temperature estimates of ~850°C by Moecher et al. (2004). Analyses of sample 08-1A yield an incredibly broad range of temperatures from ~460 to 630 °C, suggesting significant open system behavior of the rutile grains in this sample. Samples 10-4A (673 ± 20 °C) and 10-4D (598 ± 10 °C), on the other hand, yield consistent results between grains in each sample but the average values are distinct even at the 95% confidence level. Temperature estimates based on index mineral assemblages also provide an estimate of temperatures exceeding 750°C based on a metamorphic assemblage that exceeds second sillimanite-grade (Spear, 1995). The average calculated temperatures for the four samples yield a range of temperature conditions from ~500-700°C. The reason for the wide variance between the estimated temperatures and the calculated temperatures is unknown and raises questions about the reliability of the thermometer at high-pressure and/or high-temperature conditions and potential resetting of rutile during retrogression. Results from the Winding Stair Gap area seem to support findings similar to those of Chen et al. (2007), who found that analysis of rutile in ultra-high-pressure eclogites using the thermometer always generated values lower than estimates for peak metamorphism given by other thermometers and require petrographic observation in conjunction with the thermometer to detect resetting of the system.

There are three possible explanations for temperature estimates outside of anticipated ranges. The first possibility is analytical error, though we consider this the least likely explanation. Analytical conditions used on the probe are meant to account for minimum detection limits, are held constant, and are carefully calibrated against known standards. Analyses were analyzed carefully and questionable totals and concentrations from interference with other phases were discarded. Nonetheless, the electron microprobe is typically used for the analysis of major elements, and the trace element concentrations generated in this study need to be verified by ICP-MS or SIMS techniques. The other possibilities are associated with the resetting of the thermometer. Resetting could be a result of slow cooling and active deformation during prolonged regression at an elevated temperature, or could be a result of reactivation and overprinting by a later metamorphic event, such as the NeoAcadian Orogeny. Differentiating between resetting from the two causes would be exceedingly difficult. However, in either case the temperatures generated could reflect a temperature other than the peak conditions, yielding an estimate lower than expected for the highest-grade rocks. Unlike the much lower grade rocks sampled from the western Blue Ridge, the rocks at Winding Stair Gap were very likely undergoing active deformation during retrogression.

Overall, the usefulness of rutile in the generation of accurate temperature estimates for metapelitic schists appears to be roughly correlated with the metamorphic grade of the rocks. The method appears to generate reliable estimates for medium-grade metamorphic conditions, but become increasingly unreliable as rocks reach more extreme temperatures. When dealing with rocks likely reaching temperatures exceeding 700°C, the temperature estimates should be viewed as minimum values. Continued study and further analysis are necessary to investigate the cause of the observed trend and to constrain the conditions under which the thermometer is ideally useful. The method does appear valid for rocks that do not reach extreme temperatures and shows promise in helping to constrain P-T-t paths for medium-grade metamorphic rocks containing rutile.

REFERENCES

Absher, S. A., and McSween, H. Y., 1985, Granulites at Winding Stair Gap, North Carolina: The thermal axis of Paleozoic metamorphism in the southern Appalachians: *Geological Society of America Bulletin*, v. 96, p. 588–599.

Bohlen, S.R., Wall, V.J., and Boettcher, A.L., 1983, Experimental investigations and geological applications of equilibria in the system $FeO–TiO_2–Al_2O_3–SiO_2–H_2O$: *American Mineralogist,* v. 68, p. 1049–1058.

Bohlen, S.R., and Liotta, J.J., 1986, A barometer for garnet amphibolites and garnet Granulites: *Journal of Petrology*, v. 27, no. 5, p. 1025-1034.

Bream, B.R., and Hatcher, Jr., R.D., 2002, Southern Appalachians terranes amended; Timing of accretion and delimiting provenance from new detrital zircon and Nd isotopic data: *Geological Society of America Abstracts with Programs*, v. 34, n. 6.

Bream, B.R., Hatcher, Jr., R.D., Miller, C.F., and Fullagar, P.D., 2004, Detrital zircon ages and Nd isotopic data from the southern Appalachian crystalline core, Georgia, South Carolina, North Carolina, and Tennessee: New provenance constraints for part of the Laurentian margin, *in* Tollo, R.P., Corriveau, L., McLelland, J., and Bartholomew, M.J., eds., *Proterozoic Tectonic Evolution of the Grenville Orogen in North America:* Boulder, Colorado, Geological Society of America Memoir, v. 197, p. 459–475.

Butler, J.R., 1991, Metamorphism, *in* Horton, Jr., J.W., and Zullo, V.A., eds., *The Geology of the Carolinas:* Knoxville, TN, University of Tennessee Press, p. 127-141.

Carpenter, R. H., 1970, Metamorphic history of the Blue Ridge province of Tennessee and North Carolina: *Geological Society of America Bulletin*, v. 81, p. 749–761.

Carrigan, C.W., Bream, B.R., Miller, C.F., and Hatcher, R.D., 2001, Ion microprobe analyses of zircon rims from the eastern Blue Ridge and Inner Piedmont, NC-SC-GA: Implications for the timing of Paleozoic metamorphism in the southern Appalachians: *Geological Society of America Abstracts with Programs*, v. 33, n. 2.

Carrigan, C. W., Miller, C. F., Fullager, P. D., Bream, B. R., Hatcher, R. D., and Coath, C. D., 2003, Ion microprobe age and geochemistry of southern Appalachian basement, with implications for Proterozoic and Paleozoic reconstructions: *Precambrian Research*, v. 120, p. 1-36.

Chen, Z., Jinjie, Y., Li, X., and Wang, P., 2007, Application of Zr-in-rutile thermometer in the Sulu-Dabie UHP eclogites: *Acta Geologica Sinica*, v. 81, n. 10, p. 1369-1377.

Cherniak, D.J., 2000, Pb diffusion in rutile: *Contributions to Mineralogy and Petrology*, v. 139, p. 198-207.

Corrie, S.L., and Kohn, M.J., 2007, Resolving the timing of orogenesis in the Western Blue Ridge, southern Appalachians, via in situ ID-TIMS monazite geochronology: *Geology*, v. 35, p. 627-630.

Corrie, S.L., and Kohn, M.J., 2008, Trace-element distributions in silicates during prograde metamorphic reactions: Implications for monazite formation: *Journal of Metamorphic Geology*, v. 26, p. 451-464.

Deer, W.A., Howie, R.A., and Zussman, J., 1992, *An Introduction to the Rock-forming Minerals*, 2nd Edition: Longman Scientific and Technical.

Eckert, Jr., J.O. and Hatcher, Jr., R.D., 2003, Defining the Hayesville fault and terrane boundary between the western and central-eastern Blue Ridge, Georgia-North Carolina: *Geological Society of America Abstracts with Programs*, v. 35, n. 1.

Eckert, Jr., J.O., Hatcher, Jr., R.D., and Mohr, D.W., 1989, The Wayah granulite-facies metamorphic core, southwestern North Carolina: High-grade culmination of Taconic metamorphism in the southern Blue Ridge: *Geological Society of America Bulletin*, v. 101, p. 1434-1447.

Goldberg, S.A., and Dallmeyer, R.D., 1997, Chronology of Paleozoic metamorphism and deformation in the Blue Ridge thrust complex, North Carolina and Tennessee: *American Journal of Science*, v. 297, p. 488-526.

Hatcher, Jr., R.D., and Goldberg, S.A., 1991, The Blue Ridge geologic province, *in* Horton, Jr., J.W., and Zullo, V.A., eds., *The Geology of the Carolinas:* Knoxville, TN, University of Tennessee Press, p. 11-35.

Hatcher, R.D., Jr., Bream, B.R., and Eckert, J.O., Jr., 2003, Southern Blue Ridge terranes and problems with rock units, ages, and timing of events: Read the detailed geologic maps: *Geological Society of America Abstracts with Programs*, v. 35, n. 1.

Hatcher, Jr., R.D., Merschat, A.J., and Huebner, M.T., 2011, Confirmation of the Acadian-Neoacadian orogeny driven by mid-Paleozoic accretion of the Carolina superterrane in the southern-central Appalachians: *Geological Society of America Abstracts with Programs*, v. 43, n. 1, p. 159.

Hatcher, Jr., R.D., Osberg, P.H., Drake, Jr., A.A., Robinson, P., and Thomas, W.A., 1990, Tectonic map of the U.S. Appalachians, in Hatcher, R.D., Jr., et al., eds., *The Appalachian-Ouachita orogen in the United States*: Boulder, Colorado, Geological Society of America, The Geology of North America, v. F-2, scale 1:2,500,000.

Hibbard, J., 2000, Docking Carolina: Mid-Paleozoic accretion in the southern Appalachians: *Geology*, v. 28, p. 127-130.

Horton, Jr., J.W., and McConnell, K.I., 1991, The Western Piedmont, *in* Horton, Jr., J.W., and Zullo, V.A., eds., *The Geology of the Carolinas:* Knoxville, TN, University of Tennessee Press, p. 11-35.

Horton, Jr., J.W., and Zullo, V.A., 1991, An introduction to the geology of the Carolinas. *in* Horton, Jr., J.W., and Zullo, V.A., eds., *The Geology of the Carolinas:* Knoxville, TN, University of Tennessee Press, p. 1-10.

Kohn, M.J., and Malloy, M.A., 2004, Formation of monazite via prograde metamorphic reactions among common silicates: Implications for age determinations: *Geochimica et Cosmochimica Acta*, v. 68, n. 1., p. 101-113.

Li, Q., Li, S., Zheng, Y.-F., Li, H., Massonne, H.J., and Wang, Q., 2003, A high precision U-Pb age of metamorphic rutile in coesite-bearing eclogite from the Dabie Mountains in central China: A new constraint on the cooling history: *Chemical Geology*, v. 200, p. 255-265.

Luvizotto, G.L., and Zack, T., 2009, Nb and Zr behavior in rutile during high-grade metamorphism and retrogression: An example from the Ivrea-Verbano Zone: *Chemical Geology*, v. 261, p. 303-317.

Luvizotto, G.L., Zack, T., Meyer, H.P., Ludiwg, T., Triebold, S., Kronz, A., Munker, C., Stockli, D.F., Prowatke, S., Klemme, S., Jacob, D.E., and von Eynatten, H., 2009, Rutile crystals as potential trace element and isotope mineral standards for microanalysis: *Chemical Geology*, v. 261, p. 346-369.

McSween, Jr., H.Y., and Absher, B.S., 1984, Paleozoic granulite facies rocks in the thermal axis of the southern Appalachians: *Geological Society of America Abstracts with Programs*, v. 16, n. 6.

McClellan, E.A., Steltenpohl, M.G., Thomas, C., and Miller, C.F., 2007, Isotopic age constraints and metamorphic history of the Talladega Belt: New evidence for timing of arc magmatism and terrane emplacement along the southern Laurentian margin: *Journal of Geology*, v. 115, p. 541-561.

Meinhold, G., 2010, Rutile and its applications in earth sciences: *Earth-Science Reviews*, v. 102, p. 1-28.

Meinhold, G., Anders, B., Kostopoulos, D., and Reischmann, T., 2008, Rutile chemistry and thermometry as provenance indicator: An example from Chios Island, Greece: Sedimentary Geology, v. 203, p. 98-111.

Merschat, A.J., Hatcher, Jr., R.D., Bream, B.R., and Miller, C.F., 2010, Age and distribution of southern Appalachian metamorphism delimited by SHRIMP U-Pb metamorphic zircon ages: *Geochimica et Cosmochimica Acta*, v.74, n. 11, supplement 1, p. A701.

Mezger, K., Hanson, G.N., and Bohlen, S.R., 1989, High-precision U-Pb ages of metamorphic rutile: Application to cooling history of high-grade terranes: *Earth and Planetary Science Letters*, v. 96, p. 106-118.

Miller, B.V., Fetter, A.H., and Steward, K.G., 2006, Plutonism in three orogenic pulses, Eastern Blue Ridge Province, southern Appalachians: *Geological Society of America Bulletin*, v. 118, p. 171-184.

Miller, C. F., Hatcher, Jr., R. D., Ayers, J. C., Coath, C. D., and Harrison, T. M., 2000, Age and zircon inheritance of eastern Blue Ridge plutons, southwestern North Carolina and northeastern Georgia with implications for magma history and evolution of the southern Appalachian orogen: *American Journal of Science*, v. 300, p. 142–172.

Moecher, D.P., Samson, S.D., and Miller, C.F., 2004, Precise time and conditions of peak Taconian granulite facies metamorphism in the southern Appalachian orogen, USA, with implications for zircon behavior during crustal melting events: *Journal of Geology*, v. 112, p. 289-304.

Mohr, D.W., and Newton, R.C., 1983, Kyanite-staurolite metamorphism in sulfidic schists of the Anakeesta Formation, Great Smoky Mountains, North Carolina: *American Journal of Science*, v. 283, p. 97-134.

Ownby, S.E., Miller, C.F., Berquist, P.J., Carrigan, C.W., Wooden, J.L., Fullagar, P.D., 2004, U-Pb geochronology and geochemistry of a portion of the Mars Hill terrane, North Carolina-Tennessee: Constraints on origin, history, and tectonic assembly, *in* Tollo, R.P., Corriveau, L., McLelland, J., and Bartholomew, M.J., eds., *Proterozoic tectonic evolution of the Grenville orogen in North America*: Geological Society of America Memoir, v. 197, p. 609-632.

Schmitz, M.D., and Bowring, S.A., 2003, Constraints on the thermal evolution of continental lithosphere from U-Pb accessory mineral thermochronometry of lower crustal xenoliths, southern Africa: *Contributions to Mineralogy and Petrology*, v. 144, p. 592-618.

Spear, F.S., 1995, *Metamorphic Phase Equilibria and Pressure-Temperature-Time Paths*: Mineralogical Society of America.

Spear, F. S., Wark, D. A., Cheney, J. T., Schumacher, J. C., and Watson, E. B., 2006, Zr-in-rutile thermometry in blueschists from Sifnos, Greece: *Contributions to Mineralogy and Petrology, v. 152, n.* 3, p. 375-385.

Stendal, H. et al., 2006, Derivation of detrital rutile in the Yaounde region from the Neoproterozoic Pan-African belt in southern Cameroon (Central Africa): *Journal of African Earth Sciences*, v. 44, p. 443-458.

Thigpen, J.R., and Hatcher, R.D., 2009, Geologic map of the western blue ridge and portions of the eastern blue ridge and valley and ridge provinces in southeast Tennessee, southwest North Carolina, and northern Georgia: Geological Society of America.

Tomkins, H.S., Powell, R., and Ellis, D.J., 2007, The pressure dependence of the zirconium-in-rutile thermometer: *Journal of Metamorphic Geology*, v. 25, n. 6, p. 703-713.

Triebold, S., von Eynatten, H., Luvizotto, G.L., and Zack, T., 2007, Deducing source rock lithology from detrital rutile geochemistry: An example from the Erzgebirge, Germany: *Chemical Geology*, v. 244, p. 421-436.

Watson, E.B., Wark, D.A., and Thomas, J.B., 2006, Crystallization thermometers for zircon and rutile: *Contributions to Mineralogy and Petrology*, v. 151, p. 413-433.

Williams, H., and Hatcher, Jr., R.D., 1982, Suspect terranes and accretionary history of the Appalachian orogen: *Geology, v*. 10, p. 530-536.

Williams, H., and Hatcher, Jr., R.D., 1983, Appalachian suspect terranes, *in* Hatcher, R.D., Jr., Williams, H., and Zietz, I., eds., *Contributions to the Tectonics and Geophysics and Mountain Chains*: Geological Society of America Memoir, v. 158, p. 33-53.

Zack, T., von Eynatten, H., and Kronz, A., 2004a, Rutile geochemistry and its potential use in quantitative provenance studies: *Sedimentary Geology*, v. 171, p. 37-58.

Zack, T., Moraes, R., and Kronz, A., 2004b, Temperature dependence of Zr in rutile: Empirical calibration of a rutile thermometer: *Contributions to Mineralogy and Petrology*, v. 148, p. 471-488.

APPENDIX A: PHOTOGRAPHS OF FIELDWORK

ONU ID CODE	PICTURE FILE ID NUMBER	PICTURE CAPTION
APRU08-01	DSC00052.jpg	close-up of garnet rich rock at WSG, knife for scale
	DSC00053.jpg	medium zoom view of garnet rich rock at WSG, knife for scale
	DSC00054.jpg	close-up of garnet rich WSG rock with leucosome, knife for scale
	DSC00055.jpg	outcrop scale view of WSG collection site
	DSC00056.jpg	view of both sides of road at WSG showing overall outcrop
APRU08-02	DSC00061.jpg	outcrop scale view of collection site, no scale
	DSC00062.jpg	medium zoom view of collection site, small sledge for scale
	DSC00063.jpg	close-up of schist with small sledge for scale
	DSC00064.jpg	close-up of garnet mica schist with knife for scale
	DSC00065.jpg	medium zoom view of a different sample location at site, small sledge for scale
APRU08-03	DSC00057.jpg	close-up of garnet mica schist, knife for scale
	DSC00058.jpg	outcrop scale view of collection site on lake, Tim for scale
	DSC00059.jpg	medium zoom view of garnet mica schist with fold, knife for scale
	DSC00060.jpg	outcrop scale view of entire collection site showing lake and bridge
APRU08-04A	DSC00067.jpg	outcrop scale view of road cut wall, Tim for scale taking GPS location
APRU08-04B	DSC00068.jpg	outcrop scale view of entire road cut, car for scale
APRU08-04C	DSC00069.jpg	outcrop scale view of different portion of wall, Tim for scale
APRU08-05A	DSC00070.jpg	outcrop scale view of site collection location showing rock wall with Tim for scale
APRU08-05B	DSC00072.jpg	outcrop scale view of site collection wall from a different angle, Tim for scale
APRU08-05C	DSC00075.jpg	medium zoom view of schist, knife for scale
	DSC00076.jpg	close-up of mica schist, knife for scale
	DSC00077.jpg	outcrop scale view of entire road cut, car for scale
	DSC00078.jpg	outcrop scale view of wall location with different lithology, partially vegetation obscured
	DSC00080.jpg	outcrop scale view of wall location, similar to picture above
	DSC00081.jpg	outcrop scale view of wall, tree for scale
APRU08-06	No pictures	
APRU10-1	DSC05438.jpg	sample 1A collection site, close-up of rock, small sledge for scale
	DSC05440.jpg	sample 1A collection site, medium zoom, small sledge for scale
	DSC05441.jpg	sample 1A collection site, outcrop scale showing large portion of road cut

APRU10-2	DSC05443.jpg	sample 2A collection site, close-up of rock, small sledge for scale
	DSC05444.jpg	sample 2A collection site, medium zoom, small sledge for scale
	DSC05445.jpg	sample 2A collection site, outcrop scale showing large portion of road cut
APRU10-3A	DSC05448.jpg	sample 3A collection site, close-up of rock, small sledge for scale
APRU10-3B	DSC05449.jpg	sample 3A collection site, medium zoom, small sledge for scale
APRU10-3C	DSC05451.jpg	sample 3A collection site, outcrop scale showing larger portion of road cut
	DSC05452.jpg	sample 3B collection site, close-up of rock, small sledge for scale
	DSC05453.jpg	sample 3B collection site, medium zoom, small sledge for scale
	DSC05455.jpg	sample 3B collection site, outcrop scale showing second portion of road cut, Katie for scale
	DSC05456.jpg	sample 3C collection site, close-up of rock, small sledge for scale
	DSC05457.jpg	sample 3C collection site, medium zoom, small sledge for scale
	DSC05458.jpg	sample 3C collection site, outcrop scale, Chief's backpack for scale
APRU10-4	P6140224.jpg	close-up of rock at 4A collection site, small sledge for scale
	P6140225.jpg	sample 4A collection site, medium zoom, small sledge for scale
	P6140227.jpg	outcrop scale view of sample 4A collection site, Dan for scale
	P6150230.jpg	outcrop scale view of sample 4D collection site, Dan and Chief for scale
	P6150231.jpg	medium zoom view of sample 4D collection site, Dan and hammer for scale, Chief holding sample
	DSC05981.jpg	cutting dike with sample collected to left of dike, small sledge for scale
	DSC05983.jpg	close-up view showing foliation of sample collected to left of crosscutting dike, knife scale
	P6150236.jpg	medium zoom view of sample 4F collection site with crosscutting dike and clear foliation
APRU10-5	DSC06042.jpg	sample B collection site, close-up of rock, rock hammer for scale
	DSC06043.jpg	sample B collection site, outcrop scale, rock hammer as scale at sample location
	DSC06049.jpg	sample C collection site, close-up of rock, rock hammer for scale
	DSC06050.jpg	sample C collection site, outcrop scale, rock hammer for scale
	DSC06051.jpg	sample D collection site, close-up of rock covered in lichen/moss, small sledge for scale
	DSC06053.jpg	sample D collection site, outcrop scale, small sledge for scale

Photograph files are available in electronic format upon request.

APPENDIX B: GENERATING MAPS USING ARCGIS

An important part of fieldwork is recording exactly where samples are collected so that they can be interpreted within the outcrop and on a regional scale. Part of the fieldwork process required collection of GPS points using two separate GPS units. Once we returned from the field, the GPS points from the units were compared for accuracy and the finalized points were added to the ArcGIS software program. The GIS program allows the sample locations to be displayed graphically in conjunction with other information, such as rock type, transportation, state lines, etc., to create maps.

Once the GPS points were recorded in the ArcGIS program, the additional data necessary for use in conjunction with the sample locations was input. Each base map came from a digital file imported into the GIS program and georeferenced, so that points on the map with a known location and the latitude and longitude system of the ArcGIS program were aligned. Georeferencing is critical to the map-making process and allows final maps to display the correct spatial relationship between digital maps from multiple sources and the GPS locations collected in the field. The basic steps for georeferencing a map are as follows:

- Open a base map that contains the desired projection and datum, since that will set the data frame properties for the file. Also, make sure that the georeferencing toolbar is active by choosing View/Toolbars, then selecting “Georeferencing.”

- Use the add data button to add the image file/map you would like to georeference. If you get an error message saying there is missing spatial data, hit OK to continue.
- On the georeferencing toolbar, make sure that the layer you want to georeference is selected in the dropdown menu. Adjust the map view so that you can see the area of the original layer that you are working in and choose the "Fit to Display" option on the georeferencing toolbar to bring the layer that you are adding to this area.
- Click on the Add Control Point button on the georeferencing toolbar.
- You have two options for adding control points. You can either match a point on the new image with an existing point on the original image or enter known latitude and longitude coordinates. To match common points on the two maps, first click on the point on the image to be georeferenced then on the matching point on the original. It is helpful to zoom in so that you can be as precise as possible. To add specific coordinates instead, click on the location on the image being georeferenced then right click and choose the add lat/lon data. Fill in the data you know in the window that opens.
- You can change the calculation being used to fit the map to your points in the window which allows you to view all of the points you have entered. The higher the order chosen, the more the image is distorted.
- Once you are done, in the georeferencing toolbar, click "Georeferencing" then choose "Update Georeferencing" to save changes.

Four regional maps and ten detailed quadrangle maps were georeferenced over the course of the project for use along with the sample locations in mapping. The ArcGIS program has been used to produce maps showing the locations of all samples within specific terranes or isograds and to provide a regional understanding of the fieldwork locations. Figure B.1 provides an example of one of the maps produced through the ArcGIS program, showing a detailed geologic map of the locations for samples from the Blue Ridge.

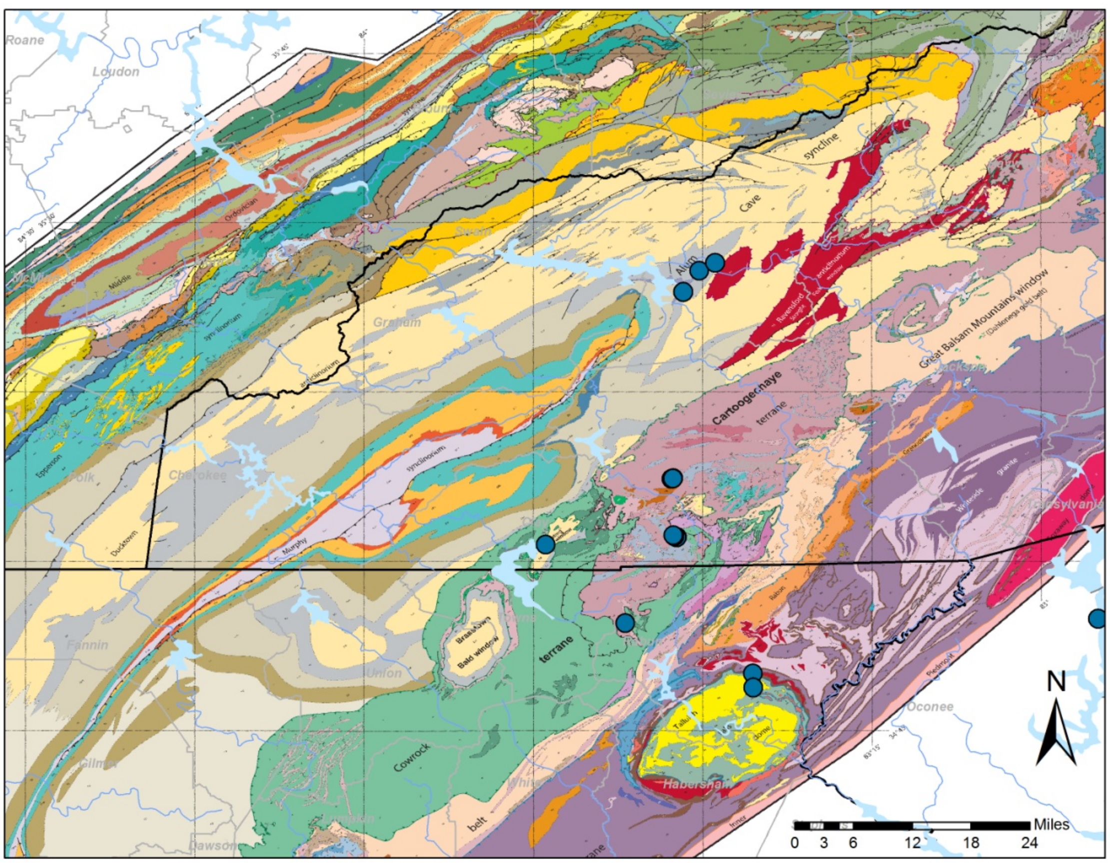

Figure B.1: Detailed geologic map of the southern Appalachians, including sample locations for the study.

APPENDIX C: THIN SECTION MAPS

Once the mineral content of the thin sections was established, the thin sections containing rutile were photographed using a Leica camera and reflected light microscope. The pictures showing portions of the slides were synthesized into complete pictures of the slides to be used as maps during electron microprobe analysis. During the electron microprobe analysis sessions, notations showing the location and identification code assigned to each analyzed grain were recorded on the grain maps created.

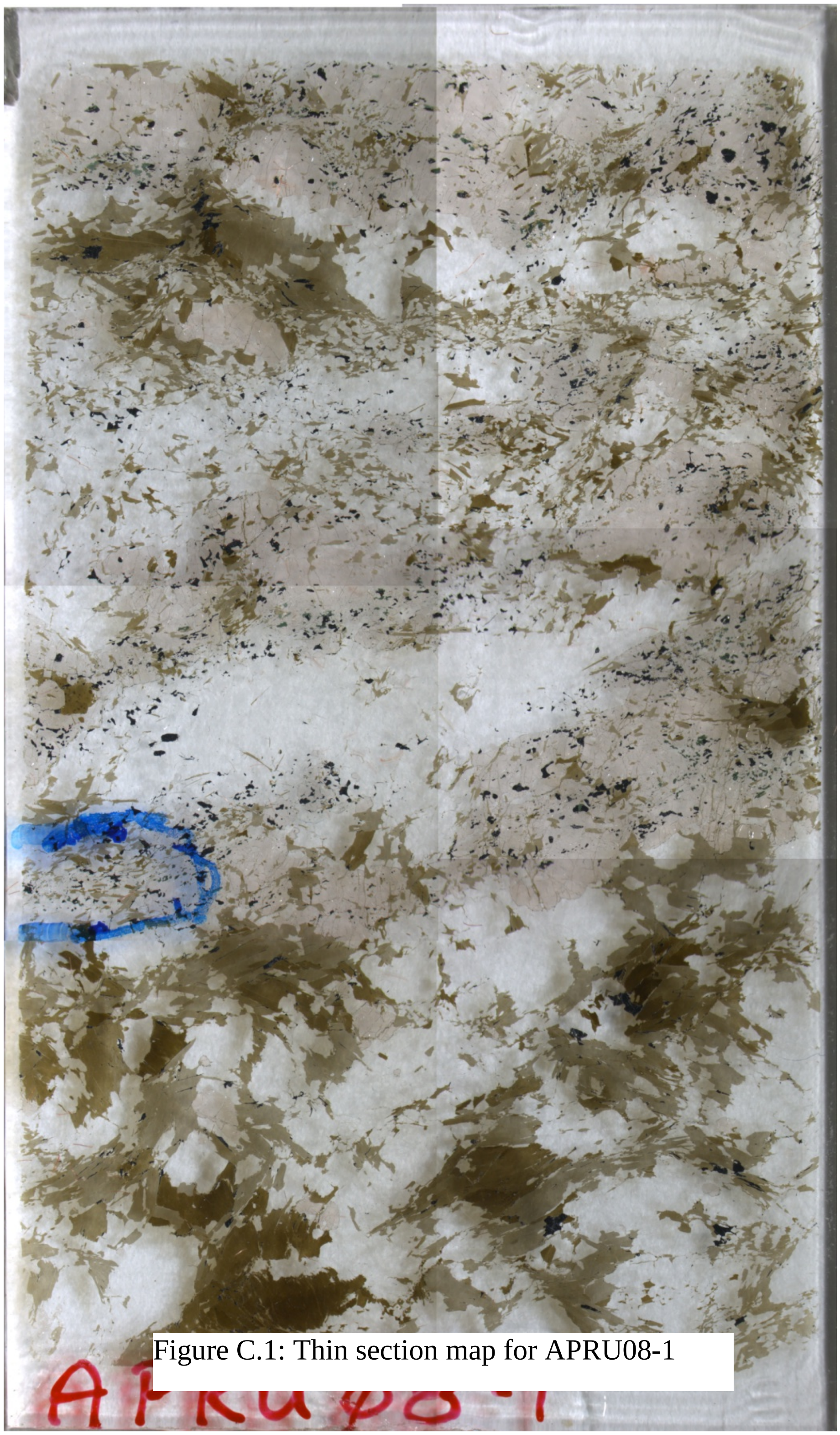

Figure C.1: Thin section map for APRU08-1

Figure C.2: Thin section map for APRU010-1A

Figure C.3: Thin section map for APRU10-1B

Figure C.4: Thin section map for APRU10-4A

Figure C.5: Thin section map for APRU10-4D

Figure C.6: Thin section map for APRU10-4E

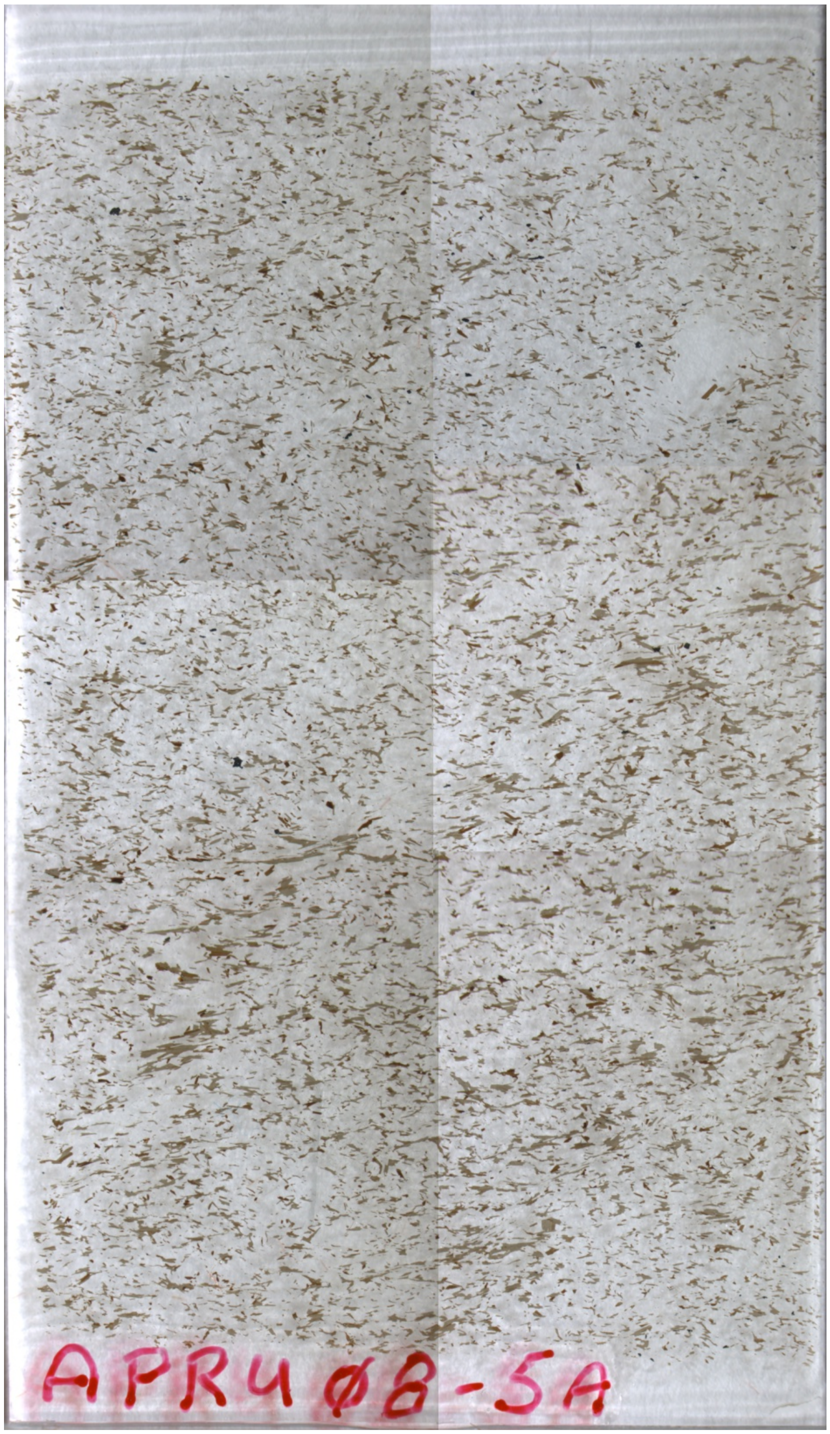

Figure C.7: Thin section map for APRU10-5A

Figure C.8: Thin section map for APRU10-5D

APPENDIX D: BSE IMAGES OF RUTILE GRAINS

The backscatter detector was used to capture BSE images for most of the rutile grains analyzed. Images were taken at normal contrast for all imaged grains, as well as at high contrast for some grains to show any banding from the inclusion of Fe-Ti oxides or textural cracks within the rutile grains. Since an image was taken for most grains analyzed, the number of BSE image files is large. Therefore, the BSE images are available electronically by request.

Folder Name	Date of Data Collection
11-aug-2010 rutile BSE	August 11-13, 2010
31-jan-2011 rutile BSE	January 31-February 3, 2011

APPENDIX E: ANALYTICAL CONDITIONS FOR THE CAMECA SX-100 EMPA

Rutile Analytical Conditions: August 2010

Common information**:**
File Name: Carrigan-Rutiles.qtiSet
File Date: Aug/12/10-3:37 PM
Column conditions:
Cond 1:
HV (kV): 25
I (nA): 200
Size (µm): 20.
Scanning: Off
RasterLength (µm): 299.11

Xtal information:

Xtal parameters:

Si Ka	Sp1	LTAP	(2d= 25.745	K= 0.00218)
Ta Ma	Sp1	LTAP	(2d= 25.745	K= 0.00218)
Zr La	Sp2	PET	(2d= 8.75	K= 0.000144)
Zr La	Sp3	LPET	(2d= 8.75	K= 0.000144)
Fe Ka	Sp4	LLIF	(2d= 4.0267	K= 0.000058)
Cr Ka	Sp4	LLIF	(2d= 4.0267	K= 0.000058)
V Ka	Sp4	LLIF	(2d= 4.0267	K= 0.000058)
Ti Kb	Sp4	LLIF	(2d= 4.0267	K= 0.000058)
Nb La	Sp5	PET	(2d= 8.75	K= 0.000144)

Pha parameters:

Elt. Line	Spec	Xtal	Bias (V)	Gain	Dtime (µs)	Blin (mV)	Wind (mV)	Mode
Si Ka	Sp1	LTAP	1297	2597	3	720	4800	Auto
Ta Ma	Sp1	LTAP	1297	2597	3	786	4734	Auto
Zr La	Sp2	PET	1293	877	3	1206	2796	Auto
Zr La	Sp3	LPET	1850	895	3	1207	2796	Auto
Fe Ka	Sp4	LLIF	1847	407	3			Inte
Cr Ka	Sp4	LLIF	1847	407	3			Inte
V Ka	Sp4	LLIF	1847	407	3			Inte
Ti Kb	Sp4	LLIF	1847	407	3			Inte
Nb La	Sp5	PET	1273	878	3			Inte

Acquisition information:

Elt. Line	Spec	Xtal	Peak	Pk Time Time/Repeat	Bg Off1	Bg Off2	Slope/IBg Range	Bg Time #Channels	Calibration	Intensity (cps/nA)
Si Ka	Sp1	LTAP	27742	30	-915	1235		15	ZIRC_SiSp1_ZrSp2_ZrSp3	1457.9
Ta Ma	Sp1	LTAP	28217	150	-1400	1800		75	Ta_TaSp1	2711.3
Zr La	Sp2	PET	69391	180	-800		0.9	180	ZIRC_SiSp1_ZrSp2_ZrSp3	69.6
Zr La	Sp3	LPET	69456	180	-800		0.9	180	ZIRC_SiSp1_ZrSp2_ZrSp3	163.7
Fe Ka	Sp4	LLIF	48096	40	-2000	1500		20	Magnetite (USNM)_FeSp4	1630.3
Cr Ka	Sp4	LLIF	56874	40	-2000	2000		20	Cr2O3_CrSp4	1334.4
V Ka	Sp4	LLIF	62186	60	-1500	2300		30	V2O5_V Sp4	963.8
Ti Kb	Sp4	LLIF	62435	10	-1758	2045		5	TIO2_TiSp4	166.7
Nb La	Sp5	PET	65292	180		600	1.02	180	Nb_NbSp5	215.8

Rutile Analytical Conditions: January 2011

Common information:
File Name: Carrigan-Rutiles.2011.qtiSet
File Date: Jan/29/11-3:54 PM
Column conditions:
Cond 1:
HV (kV): 20
I (nA): 200
Size (μm): 20.
Scanning: Off
RasterLength (μm): 149.42

Xtal information:

Xtal parameters:

Si Ka	Sp1	LTAP	(2d= 25.745	K= 0.00218)
Ta Ma	Sp1	LTAP	(2d= 25.745	K= 0.00218)
Zr La	Sp2	PET	(2d= 8.75	K= 0.000144)
Zr La	Sp3	LPET	(2d= 8.75	K= 0.000144)
Fe Ka	Sp4	LLIF	(2d= 4.0267	K= 0.000058)
Cr Ka	Sp4	LLIF	(2d= 4.0267	K= 0.000058)
Ti Kb	Sp4	LLIF	(2d= 4.0267	K= 0.000058)
Nb La	Sp5	PET	(2d= 8.75	K= 0.000144)

Pha parameters:

Elt. Line	Spec	Xtal	Bias (V)	Gain	Dtime (μs)	Blin (mV)	Wind (mV)	Mode
Si Ka	Sp1	LTAP	1293	2584	3			Inte
Ta Ma	Sp1	LTAP	1293	2584	3			Inte
Zr La	Sp2	PET	1297	878	3			Inte
Zr La	Sp3	LPET	1844	878	3			Inte
Fe Ka	Sp4	LLIF	1836	386	3			Inte
Cr Ka	Sp4	LLIF	1836	386	3			Inte
Ti Kb	Sp4	LLIF	1836	386	3			Inte
Nb La	Sp5	PET	1272	884	3			Inte

Acquisition information:

Elt. Line	Spec	Xtal	Peak	Pk Time Time/Repeat	Bg Off1	Bg Off2	Slope/IBg Range	Bg Time	Calibration #Channels	Intensity (cps/nA)
Si Ka	Sp1	LTAP	27735	30	-915	1235		15	ZIRC_SiSp1_ZrSp2_ZrSp3	1441.2
Ta Ma	Sp1	LTAP	28211	150	-1400	1800		75	Ta_TaSp1	2626.6
Zr La	Sp2	PET	69403	180	-800		0.9	180	ZIRC_SiSp1_ZrSp2_ZrSp3	62.4
Zr La	Sp3	LPET	69454	180	-800		0.9	180	ZIRC_SiSp1_ZrSp2_ZrSp3	147.0
Fe Ka	Sp4	LLIF	48081	80	-2000	1500		40	Magnetite (USNM)_FeSp4	1138.0
Cr Ka	Sp4	LLIF	56869	80	-2000	2000		40	Cr2O3_CrSp4	896.9
Ti Kb	Sp4	LLIF	62434	20	-1758	2045		10	TIO2_TiSp4	109.0
Nb La	Sp5	PET	65297	180		600	1.02	180	Nb_NbSp5	146.0

APPENDIX F: FULL NORMALIZED RUTILE DATA FROM EMPA ANALYSIS

The rutile data was normalized using a template created in Microsoft Excel. Two different files containing normalization data were created, one for each of the two trips to the University of Michigan. Each of the files contains the normalized rutile data, on the rutile spreadsheet tab. The files also contain the necessary data and the plots of the Zr-in-rutile temperature histograms, Cr vs. Nb, and the zirconium-in-rutile temperature vs. iron content for each of the trips on their respective labeled spreadsheets within the file as a whole. Excel files are available electronically upon request.

File Name	Date of Data Collection
11-aug-2010 rutile norm.xlsx	August 11-13, 2010
31-jan-2011 rutile norm.xlsx	January 31-February 3, 2011

APPENDIX G: PRESENTATION OF RESULTS

October 22, 2010- Oral presentation of preliminary results to geology students and faculty to fulfill a portion of the Pence Boyce summer research requirements.

October 29, 2010- Presentation of a poster covering preliminary results to fulfill a portion of the Pence Boyce summer research requirements.

October 31, 2010- Oral presentation of the initial results at the annual Geological Society of America meeting in Denver, Colorado for approximately fifty geology professionals. The abstract for the presentation was published in the Geological Society of America Abstract with Programs.

Eccles, K.A., and Carrigan, C.W., 2010, Preliminary P-T-t investigation of rutile-bearing pelitic schists in the southern Appalachian Blue Ridge: Geological *Society of America Abstracts with Programs*, v. 42. n. 5, p. 48.

2010 GSA Denver Annual Meeting (31 October –3 November 2010)

Paper No. 12-4

Presentation Time: 9:05 AM-9:20 AM

PRELIMINARY P-T-T INVESTIGATION OF RUTILE-BEARING PELITIC SCHISTS IN THE SOUTHERN APPALACHIAN BLUE RIDGE

ECCLES, Kathryn A. and CARRIGAN, Charles W., Dept. of Physical Sciences, Olivet Nazarene University, One University Avenue, Bourbonnais, IL 60914, keccles@live.olivet.edu

Over the past decade, geochronology studies in the southern Appalachians have focused on zircon, monazite, and mica ages to confirm the occurrence of a major Taconic event (~460-450 Ma) affecting the Western and Central Blue Ridge, followed by a younger NeoAcadian (~360-345 Ma) event affecting the Eastern Blue Ridge and Piedmont. Peak conditions of granulite facies metamorphism are estimated at ~850°C (garnet-biotite) and 7-9 kbar (GASP) for sillimanite schists at Winding Stair Gap (WSG), but thermobarometric studies of metasedimentary rocks in the region are limited and consequently P-T-t-D paths are poorly understood. Further, relating zircon U-Pb dates to petrologic context is challenging, adding complexity to the interpretation of the ages. Many details of the orogenic processes in the region remain unanswered, such as the depth of burial, rates of burial, cooling, & exhumation of various terranes, and variation of ages along strike. Rutile provides a robust, high-temperature U-Pb geochronometer that forms during metamorphic reactions and is a key phase for applying several thermobarometers (e.g., GRAIL, GRIPS) in the determination of P-T conditions. We have begun a study of rutile-bearing metapelitic schists in the Blue Ridge, and our goal is to obtain U-Pb isotopic and trace element analyses on rutile for age constraints as well as major element mineral data for thermobarometric constraints; here we report initial results of our investigation. Initial sampling indicates that rutile-bearing schists are somewhat sparse across the orogen, but have been confirmed in the Great Smoky Group of the Western Blue Ridge as well as in the Cartoogechaye & Cowrock terranes of the Central Blue Ridge, all of which were metamorphosed to high grades during the Taconic Orogeny. Rutile is found in both kyanite- and sillimanite-grade rocks, primarily as a matrix phase associated with biotite. Common assemblages in these rocks include garnet, biotite, muscovite, quartz, opaques, plagioclase, ±kyanite, ±sillimanite, and ±staurolite. Rutile is especially common in the shooting creek schist and in lithologies at Winding Stair Gap.

2010 GSA Denver Annual Meeting (31 October –3 November 2010)
General Information for this Meeting

Session No. 12
High-Pressure and High-Temperature Metamorphism: *P–T–t* Paths and Tectonics
Colorado Convention Center: Room 203
8:00 AM-12:00 PM, Sunday, 31 October 2010

Geological Society of America *Abstracts with Programs*, Vol. 42, No. 5, p. 48

March 2011- Oral presentation of final results and oral exam to fulfill requirements for Departmental Honors in Geoscience.

April 2011- Participation in Scholar’s Week and oral presentation of final results in an open forum at Olivet Nazarene University.